AN ABSTRACT OF THE THESIS OF

Jeffery R. Hughes for the degree of Master of Science in Electrical and Computer Engineering presented on December 9, 2003.

Title: Adaptive Digital Transceiver for Rayleigh Fading Channels

Abstract Approved:

_____

Mario E. Magaña

This thesis presents an adaptive modulation scheme using a Walsh-code modulator. The Walsh-code modulator consists of a dynamic demultiplexer and predetermined sets of orthogonal Walsh-Hadamard codes. The demultiplexer can de-multiplex the input bit stream into a maximum of thirty-two sub-streams. The Walsh-Hadamard codes are used to spread the spectrum of the demultiplexed sub-streams. The Walsh-code modulator produces a multi-level pulse amplitude modulated (PAM) signal by summing the spread sub-streams. The number of levels contained in the constellation of the PAM signal varies, based on the number of demultiplexed sub-streams. The error rate performance of different constellations produced by the Walsh-code modulator, differ when transmitted through a Rayleigh fading plus additive white Gaussian noise (AWGN) channel. As the level of fading experienced in the channel fluctuates, a desired level of error rate performance can be maintained by switching constellations, while trying to use the maximum number of sub-streams, or links, to transmit the data. Simulation results show the performance of several

constellations when transmitted through an AWGN channel and a Rayleigh fading plus AWGN channel. Also, mapping of the PAM signal onto a quadrature amplitude modulation (QAM) constellation, in order to improve the performance of the system is discussed. It is found that for a Rayleigh fading plus AWGN channel, at a given error performance level, the amount of gain in signal-to-noise ratio (SNR), from the largest constellation to the smallest constellation, is 8dB for the symbol error rate (SER) and 14dB for the bit error rate (BER).

Adaptive Digital Transceiver for Rayleigh Fading Channels

by
Jeffery R. Hughes

A THESIS

submitted to

Oregon State University

in partial fulfillment of
the requirements for the
degree of

Master of Science

Presented December 9, 2003
Commencement June 2004

Master of Science thesis of Jeffery R. Hughes presented on December 9, 2003.

APPROVED:

_____

Major Professor, representing Electrical and Computer Engineering

_____

Director of the School of Electrical Engineering and Computer Science

_____

Dean of the Graduate School

I understand that my thesis will become part of the permanent collection of Oregon State University libraries. My signature below authorizes release of my thesis to any reader upon request.

_____

Jeffery R. Hughes, Author

TABLE OF CONTENTS

LIST OF FIGURES

LIST OF FIGURES (Continued)

LIST OF FIGURES (Continued)

LIST OF APPENDICES

LIST OF APPENDIX FIGURES

Adaptive Digital Transceiver for Rayleigh Fading Channels

1 Introduction

In direct, peer-to-peer communications, the wireless channel between the transmitter and receiver can change over time, either improving or degrading the reliability of the communication. With the goal being to receive the transmitted signal with minimal errors, the communication system must take into account this variability of the channel. One approach to ensure minimal errors, is to determine the worst performance across the channel and then design the system to have the desired bit error rate (BER) in this scenario. This can be achieved by increasing the transmitted power to a level that provides the desired performance or by adding elements such as error correction coding and interleaving to the system. If the channel conditions which cause the worst performance do not occur at all times, then a system designed in the above manner is not the most efficient possible. When the channel is not performing poorly, it achieves a BER that is better than necessary by expending too much transmitted and computational power. A more efficient approach would be to allow the transmitter to adjust to the conditions of the channel. This adaptive approach has been offered as providing a solution to increasing efficiency while achieving desired performance (Torrance, et al. 1996; Goldsmith, et al. 1998).

In recent years, there have been many works concerned with adaptive modulation techniques that improve spectral efficiency and throughput, while

achieving a desired level of performance in a Rayleigh fading environment. The techniques used vary from changing the number of levels used in a modulation scheme like quadrature amplitude modulation (QAM), to using a combination of adaptive system parameters, such as the transmit power, the symbol transmit rate, the application of coding techniques to the modulation scheme, and varying the number of constellation levels. Most of the designs presented in the literature are concerned with increasing the spectral efficiency and thus, the throughput of the system. The approaches presented in the literature show that definite gains can be achieved utilizing the techniques listed above (Webb, et al. 1995; Armanious, et al. 2003; Goldsmith, et al. 1998).

Presented in this thesis is a modulation scheme that lends itself to direct use in an adaptive modulation system. The technique uses a Walsh-code modulator that can maintain a constant level of performance in a varying channel by increasing or decreasing the size of the transmitted constellation while maintaining a constant average transmitted power. This is achieved through the use of a dynamic demultiplexer which demultiplexes the input data stream into multiple sub-streams. The demultiplexed sub-streams are then spread by orthogonal Walsh-Hadamard codes and finally, summed together to produce a multi-level pulse amplitude modulation (PAM) signal. The number of demultiplexed sub-streams, or links, determines the number of levels contained in the constellation of the PAM signal, which determines the performance of the transmitted signal through the channel. Since, QAM is a more robust system when using constellations with more than four levels and because there

have been many works on adaptive QAM and constellations designed for Rayleigh fading, mapping the PAM signal onto a QAM constellation is considered (Haykin 1988).

The following chapters describe the design and methodology of this approach and how it provides adaptability to the peer-to-peer communication environment. First, a description of the Walsh-code modulator is presented, and then the performance of transmitting the PAM signal output through an additive white Gaussian noise (AWGN) channel and a Rayleigh fading plus AWGN channel is examined. Next, is a discussion of how to improve the efficiency and performance of the system by mapping the PAM signal onto a QAM constellation. The results presented will reveal how the Walsh-code modulator can provide a communications system with the ability to adapt to the condition of the channel.

2   Walsh-code Modulator

This chapter describes the design of the Walsh-code modulator and the

characteristics of the PAM signal that it generates. The performance of the PAM

signal in channels with AWGN and Rayleigh fading plus AWGN is presented.
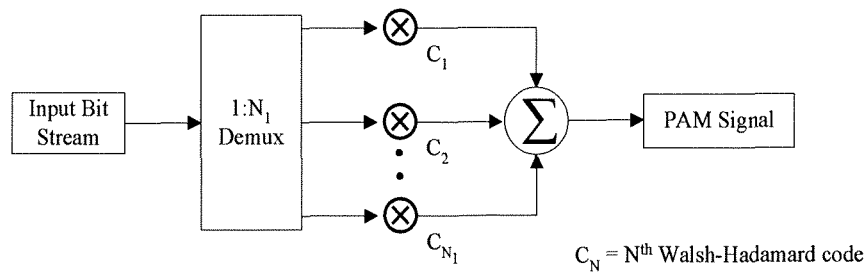
Figure 2.1
Walsh-code modulator

2.1   Walsh-code Modulator Design

A brief overview of the operation of the Walsh-code modulator is presented in

this section. A more detailed description of the Walsh-code modulator and the

simulation setup of a baseband PAM system incorporating the Walsh-code modulator

is presented in appendix A. The first operation that takes place, is the demultiplexing

of the input bit stream into N_1 sub-streams. Next, the sub-streams are made

orthogonal to each other by spreading them with orthogonal Walsh-Hadamard codes.

Lastly, the orthogonal sub-streams are summed together on a chip-by-chip basis, producing a multi-level PAM signal as output. The number of levels in the output PAM constellation equals the number of demultiplexed sub-streams plus one. For example, when $N_1=7$, the number of PAM levels produced is 8, and when $N_1=8$, the number of PAM levels produced is 9. Therefore, when N_1 is even, the number of PAM levels produced is odd, including the 0 level. When N_1 is odd, the number of PAM levels is even, excluding the 0 level. The levels in the PAM constellation produced by the Walsh-code modulator occur with a Gaussian-like probability distribution centered at zero, as shown in figures 2.2 through 2.5.
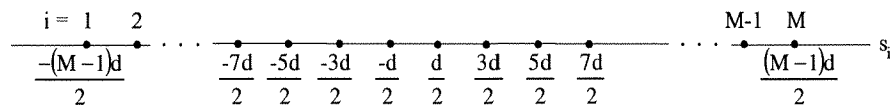
Figure 2.2
Graphical representation of the PAM constellation
produced when N_1 is odd valued
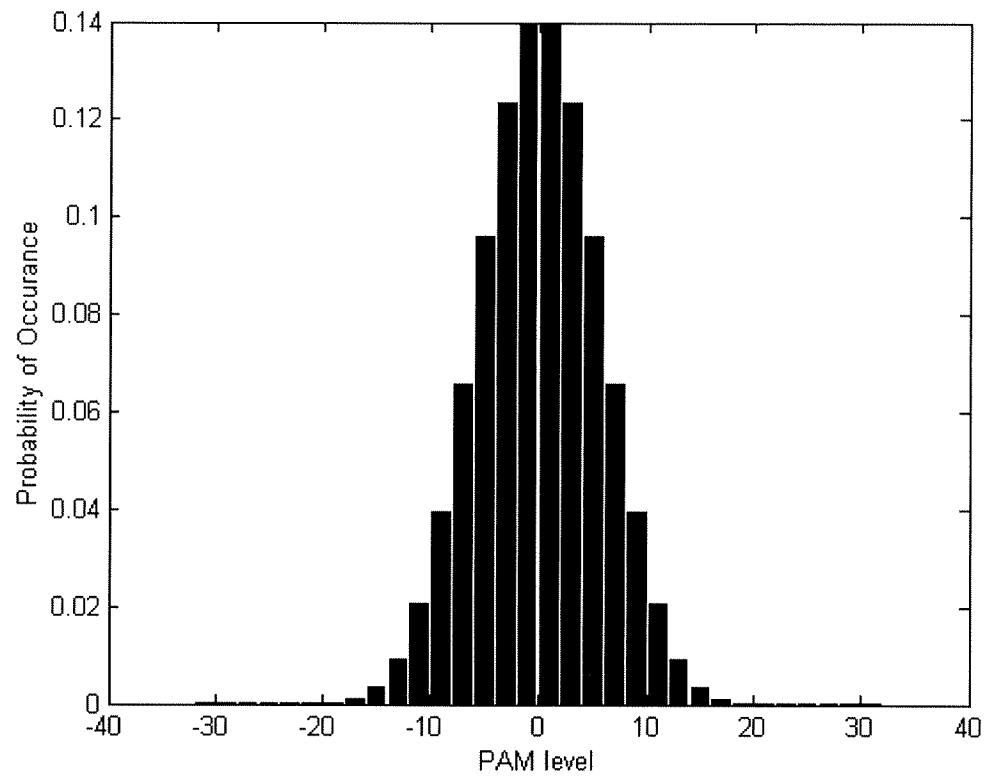
Figure 2.3
Probability distribution of the PAM levels produced with $N_1 = 31$
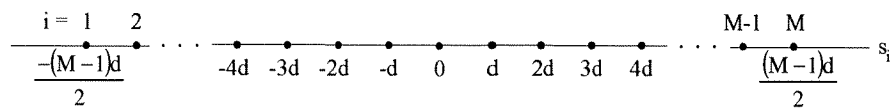
Figure 2.4
Graphical representation of the PAM constellation
produced when N_1 is even valued
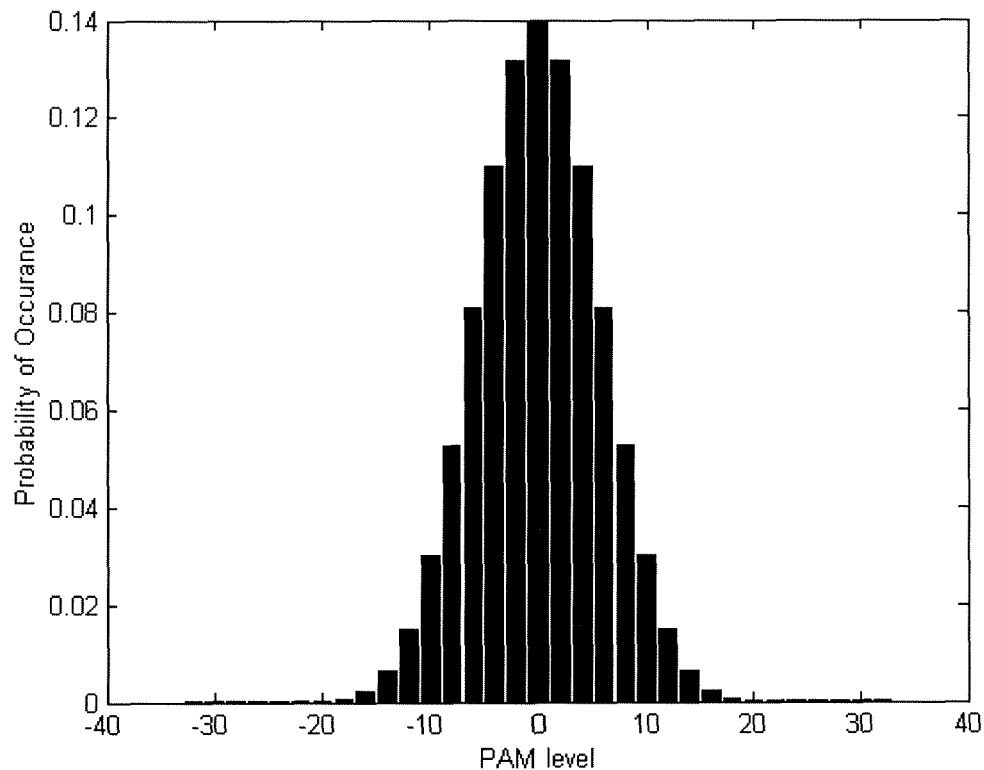
Figure 2.5
Probability distribution of the PAM levels produced with $N_1 = 32$

The Walsh-code modulator uses Walsh-Hadamard codes of length $N_2 = 8$, 16, or 32. This means that the number of demultiplexed sub-streams, N_1, can vary from 5-8 when using the length 8 codes, from 9-16 when using the length 16 codes, and from 17-32 when using the length 32 codes. When the value of N_1 is equal to the length of the orthogonal code, the output symbol rate (R_c) is equal to the input bit rate (R_b). When the number of demultiplexed sub-streams is less than the length of the

orthogonal code, the symbol, or chip rate, is proportional to the input bit rate described

by

$$R_c = (N_2 * R_b)/N_1 \qquad (2.1)$$

Due to the use of demultiplexed sub-streams, a bit sequence used to estimate

the current conditions of the channel can be inserted along with the input data. One of

the links, and the corresponding Walsh-Hadamard code, can be devoted to sending the

channel estimation sequence. The throughput of the system will be reduced as a

consequence of introducing this sequence along with the input data.

2.2 Expected Performance of the PAM Signal

Appendix B provides a framework for determining the expected symbol error rate

(SER) performance of the PAM signal produced by the Walsh-code modulator, in

channels with AWGN and Rayleigh fading plus AWGN. Knowing how the PAM

system should perform confirms that the simulation is calibrated correctly. The results

in appendix B apply to a PAM constellation that has an odd number of levels with a

Gaussian probability distribution. Therefore, the following figures only provide

comparisons with simulation results of constellations produced when N_1 is even

valued.

Equation 2.2 calculates the expected performance in an AWGN channel.

$$P_{se} = 1 - p_1 + p_2 Q\left(\sqrt{\frac{E_{av}}{KN_0}}\right) \tag{2.2}$$

$$p_1 = P\{s_0\} + 2P\{s_1\} + 2\sum_{i=2}^{\frac{M-1}{2}} P\{s_i\} \tag{2.3}$$

$$p_2 = 2P\{s_0\} + 2P\{s_1\} + 4\sum_{i=2}^{\frac{M-1}{2}} P\{s_i\} \tag{2.4}$$

$$K = \sum_{i=2}^{\frac{M-1}{2}} \left((2i - 1 - M)^2 P\{s_i\}\right) \tag{2.5}$$

Where P_{se} is the probability of symbol error, E_{av} is the average PAM symbol energy, M is the total number of PAM symbols, and s_i is the ith PAM symbol.

Figure 2.6 compares the expected performance to simulation results in AWGN for values of N_1 = 8, 16, and 32. The SER found through simulation closely matches the expected results calculated using equation 2.2. Therefore the simulation is correctly calibrated.
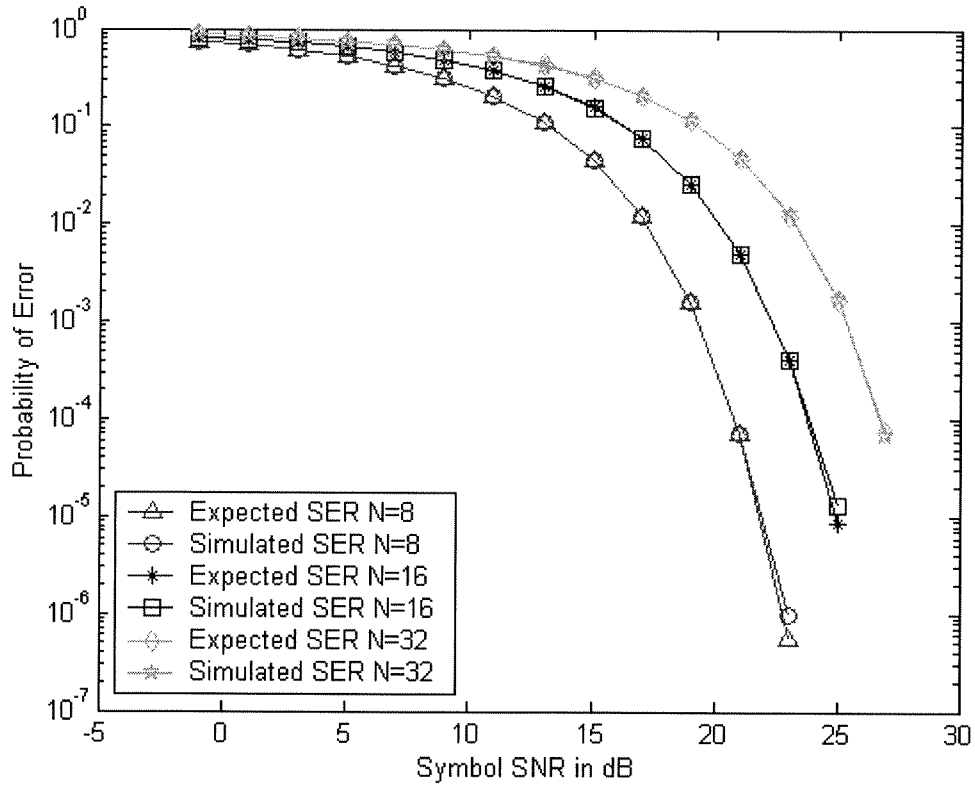
Figure 2.6
Expected PAM SER verses simulated PAM
SER in AWGN for $N_1 = 8, 16, 32$

Equation 2.6 gives the expected performance in a Rayleigh fading plus AWGN channel.

$$P_{se} \leq 1 - p_1 + \frac{1}{2} p_2 \left[1 - \sqrt{\frac{\gamma}{\gamma + 2K}} \right] \qquad (2.6)$$

$$p_1 = P\{s_0\} + 2P\{s_1\} + 2\sum_{i=2}^{\frac{M-1}{2}} P\{s_i\} \qquad (2.7)$$

$$p_2 = 2P\{s_0\} + 2P\{s_1\} + 4\sum_{i=2}^{\frac{M-1}{2}} P\{s_i\}$$
(2.8)

$$K = \sum_{i=2}^{\frac{M-1}{2}} \left((2i - 1 - M)^2 P\{s_i\} \right)$$
(2.9)

$$\gamma = \frac{E_{av}}{N_0} E\{\alpha^2\} = \frac{2\sigma^2 E_{av}}{N_0}$$
(2.10)

Figure 2.7 compares the expected performance to simulation results in Rayleigh fading plus AWGN, for values of $N_1 = 8$, 16, and 32. The SER found through simulation is close to the expected results calculated using equation 2.6. Therefore the simulation is correctly calibrated.
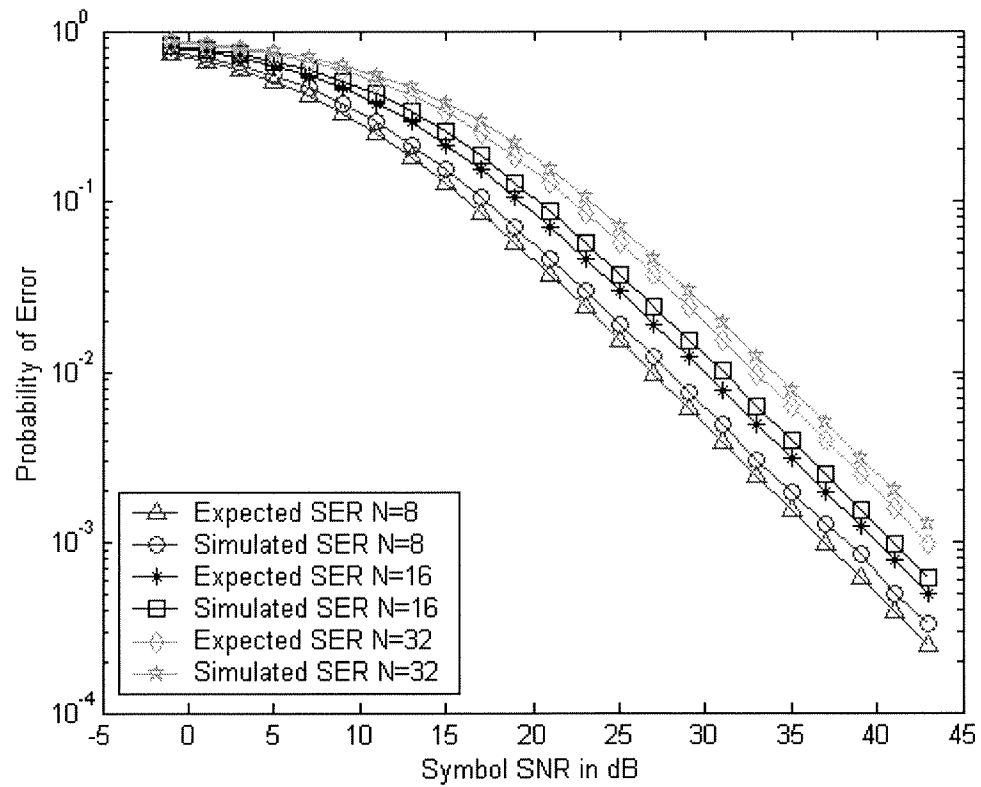
Figure 2.7
Expected PAM SER verses simulated PAM SER in
Rayleigh fading plus AWGN for N1 = 8, 16, 32

2.3 Simulation Setup

Simulation of a baseband PAM system utilizing the Walsh-code modulator is

used to determine the performance of the PAM output from the Walsh-code modulator

through an AWGN channel and a Rayleigh fading plus AWGN channel.

```
┌─────────────────────┐  {b_m}   ┌─────────────────────────────┐
│  INPUT BIT STREAM   │ ───────▶ │  WALSH-CODE MODULATOR       │
│      {b_m}          │          │  Output PAM Signal, {s_i}   │
└─────────────────────┘          └─────────────────────────────┘
                                                    │
                                               {s_i}│
                                                    ▼
                                   ┌──────────────────────────────────────────────┐
                                   │              CHANNEL                           │
                                   │  For AWGN:  r_m = s_i + w_m                     │
                                   │  For Rayleigh Fading Channel with AWGN:        │
                                   │                        r_m = αs_i + w_m         │
                                   └──────────────────────────────────────────────┘
                                                    │
                                               {r_m}│
                                                    ▼
┌─────────────────────┐ {b̃_m}  ┌────────────────────────────┐ {s̃}  ┌──────────────────────────────────┐
│  OUTPUT BIT STREAM  │◀────────│  DEMODULATOR                │◀──────│  DETECTOR                        │
│      {b̃_m}          │         │  Output Bit Sequence, {b̃_m} │       │  Output Estimated Symbol, {s̃}    │
└─────────────────────┘         └────────────────────────────┘       └──────────────────────────────────┘
```
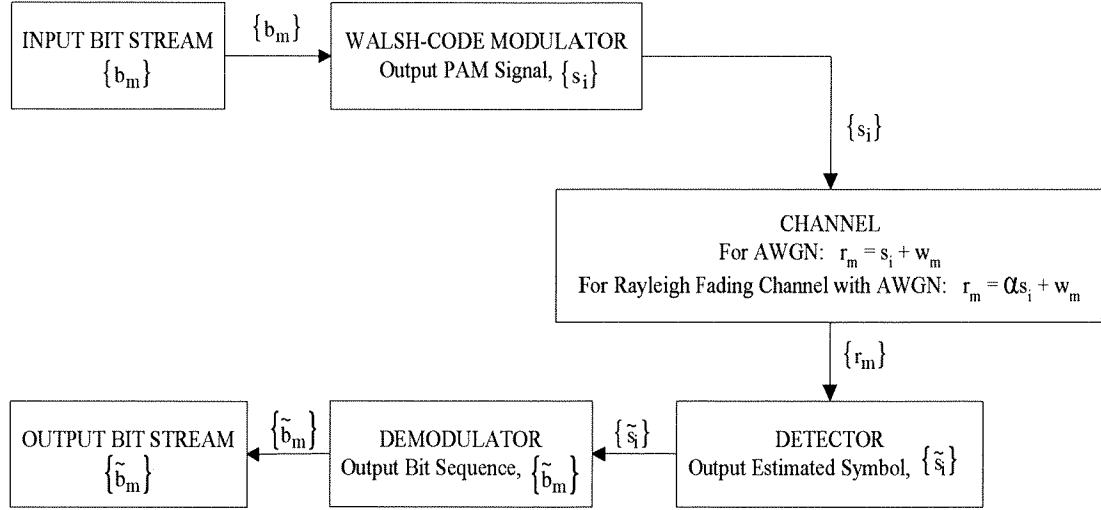
Figure 2.8
Baseband PAM system block diagram

For transmission through the channel, the energy of the PAM signal must be scaled to have the appropriate energy, as determined by the input bit energy. The determination of the value of this scaling factor is presented in appendix A, section A.5.

In the baseband model used for simulation of the PAM system, the AWGN present in the channel is modeled as a white noise process with power spectral density (N_0), having a Gaussian distribution with zero mean and variance $\frac{N_0}{2}$. N_0 has a value of 10^{-11}. Therefore, the received signal (r) consists of the transmitted signal plus the noise (w), represented in equation 2.11.

$$r_m = s_i + w_m \qquad (2.11)$$

14

The Rayleigh fading channel is modeled with independent fading coefficients, which are a multiplicative component (α) applied to the transmitted signal as shown in the following equation.

$$r_m = \alpha s_i + w_m \qquad (2.12)$$

The fading coefficients have a Rayleigh distribution and are characterized by the following equations.

$$f(\alpha) = \frac{\alpha}{\sigma^2} e^{\left(\frac{\alpha^2}{2\sigma^2}\right)} \qquad (2.13)$$

$$E\{\alpha\} = \sqrt{\frac{\pi}{2}}\sigma \qquad (2.14)$$

$$E\{\alpha^2\} = 2\sigma^2 \qquad (2.15)$$

The fading coefficients are normalized, so that $E\{\alpha\}=1$, therefore, $\sigma = \sqrt{\frac{2}{\pi}}$.

The fading coefficients are generated using two Gaussian random variables (x, y) with variance σ^2. The generation of α is shown below (Roden 1996).

$$\alpha = \sqrt{x^2 + y^2} \qquad (2.16)$$

At the receiver, maximum-likelihood symbol detection is performed using a minimum Euclidean distance metric that determines which constellation point the received signal is closest to. Equation 2.17 shows the metric used (Haykin 1988; Boutros, et al. 1996).

$$d = \|r_m - s_i\|^2 \qquad (2.17)$$

For the case of an AWGN channel, in order to recover the originally transmitted signal, the received symbols are compared to the constellation used to transmit the signal, and the constellation point closest to the received symbol is declared to be the transmitted symbol. Similarly, for the case of a Rayleigh fading plus AWGN channel, to recover the original signal, each received symbol is compared to the constellation used to transmit the signal after it has been compressed by the fading channel coefficient corresponding to the interval for that received symbol. Once again, the constellation point closest to the received symbol is declared to be the transmitted symbol. (Boutros, et al. 1996; Viterbo, et al. 1999)

After the transmitted symbols have been determined, demodulation of the received symbols takes place in order to recover the transmitted bits. Demodulation is performed by despreading a block of N_2 received symbols, using the same orthogonal codes used to spread the original sub-streams. To recover the transmitted bit sequence, the block of N_2 symbols is multiplied by each Walsh-Hadamard code used to spread the signal, and then divided by the length of the Walsh-Hadamard code.

An alternative approach to using the despreading process to recover the transmitted bits, would be to consult a table with entries that include all the possible demultiplexed bit sequences that are spread and summed together and their corresponding PAM output. Then, at the detector, the received PAM signal is compared to the table and the entry with the most symbols that match the received signal is declared to be the transmitted signal. Then, the bit sequence that corresponds to this PAM signal is the output. This method reduces the number of bit errors, since

only a subset of all the possible combinations of the PAM symbols are actually

transmitted. Therefore, if an error occurs that causes the received PAM signal to lie

outside the set of possible transmitted PAM signals, then it is highly likely that this

error can be corrected by using the table. The bit error improvement using the table

can be seen in figure 2.9.
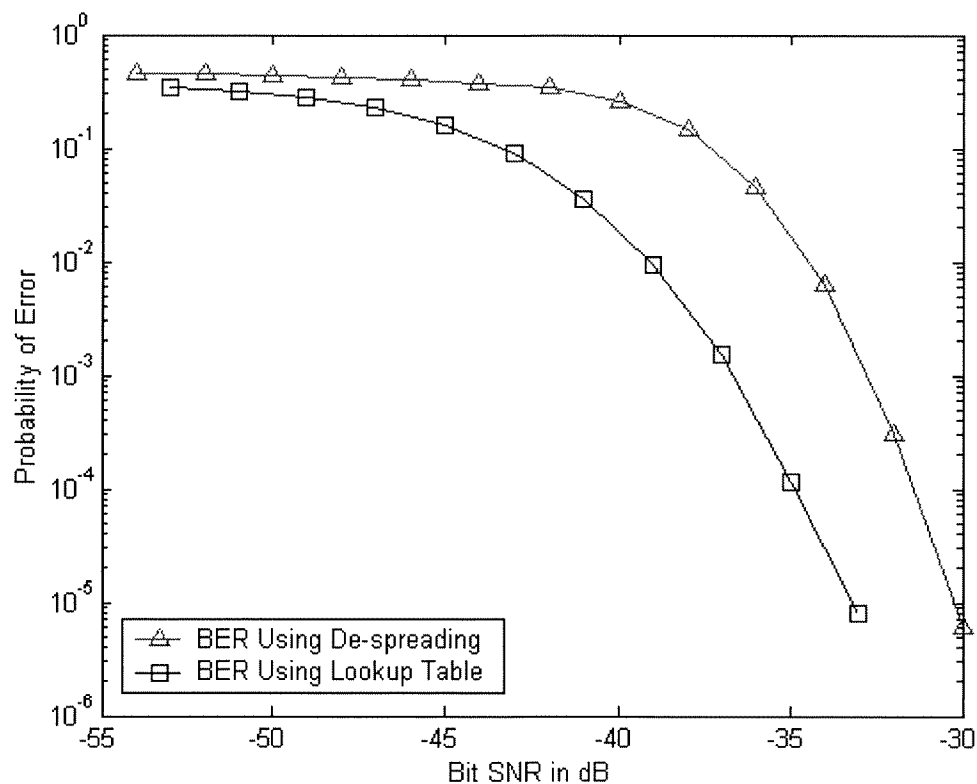
Figure 2.9
Comparison of detection using the despreading technique versus
detection using the lookup table technique, in AWGN with $N_1=8$

Unfortunately, although this method improves the bit error rate, it is a resource intensive approach and causes a significant delay in the output data. It is resource intensive because of the number of entries that must be stored in the lookup table. Above $N_1=8$, which has 512 entries, the number of required entries grows very rapidly. Once there is a large number of entries that must be searched through to find the closest match to the received signal, the amount of processing power and time necessary to complete the operation becomes prohibitive. Therefore, this approach was not adopted for use in this system.

2.4 PAM System Performance in AWGN and Rayleigh fading plus AWGN

This section presents representative examples of the performance obtained through simulation. Figure 2.10 shows the SER performance of the PAM system in AWGN. The curves show that the smallest constellation size, corresponding to $N_1 = 5$, has better performance than the increasingly larger constellations at a given SNR. Also, the amount of SER improvement between constellations decreases as the constellations get larger. This is evident in how the curves become compressed with the larger constellations. The reason the smaller constellations have better performance is because, for a given average transmit energy, the transmit energy is spread over fewer symbols than a larger constellation thus allowing for more separation between constellation points which translates into better performance. Note

that all possible constellations are not represented in the figures. This is done to

highlight the above characteristics and to simplify simulation and data gathering.
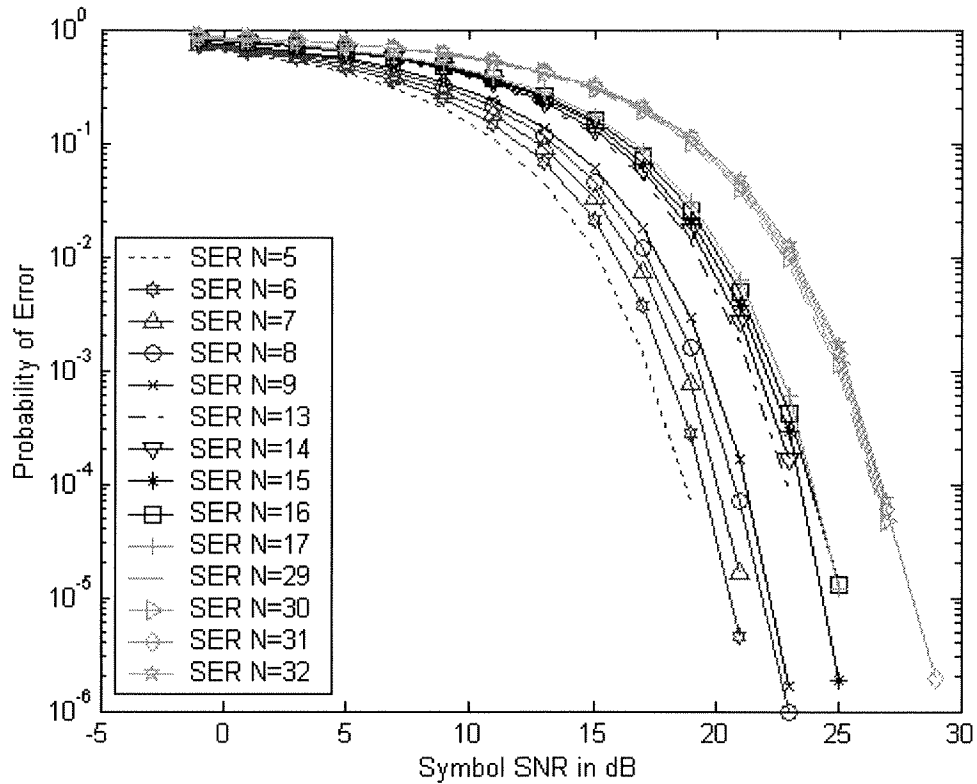
Figure 2.10
SER results for simulation of PAM system in AWGN

Figure 2.11 shows the BER performance of the PAM system in AWGN. The

same trends present in the previous SER figure are also present in the BER results.

There are noticeable jumps in the BER between constellations generated by using N_1

= 8, 9 and N_1 = 16, 17. The curves are not distributed smoothly as with the SER

curves. This is due to the fact that when switching from a Walsh-Hadamard spreading code having 8 chips with $N_1 = 8$ to a spreading code having 16 chips with $N_1 = 9$, there are 16 symbols used to transmit 9 bits of information. With the extra 7 symbols comes the extra chance that one of them might be in error and thus cause an error in the received bits. This fact causes there to be a significantly higher BER between the constellations generated by $N_1 = 8$, 9 and $N_1 = 16$, 17.
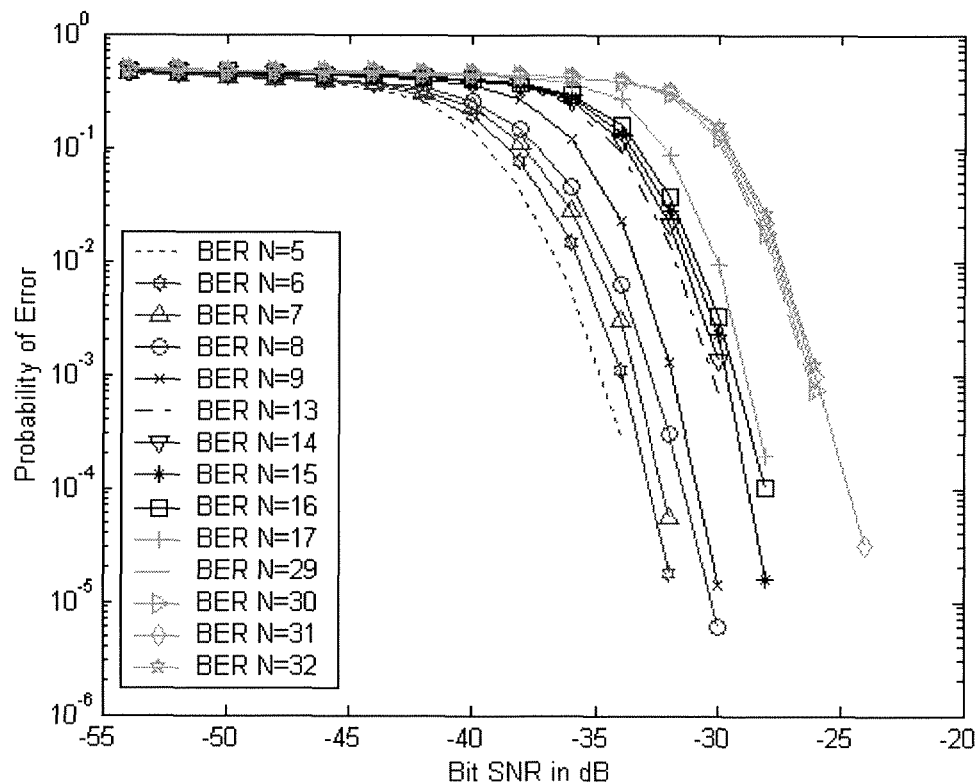
Figure 2.11
BER results for simulation of PAM system in AWGN

Figure 2.12 shows the SER performance of the PAM system in Rayleigh

fading plus AWGN. The same trends present in the previous SER figure are also

present in these results. There is a noticeable drop in performance when transmitting

through the fading channel.
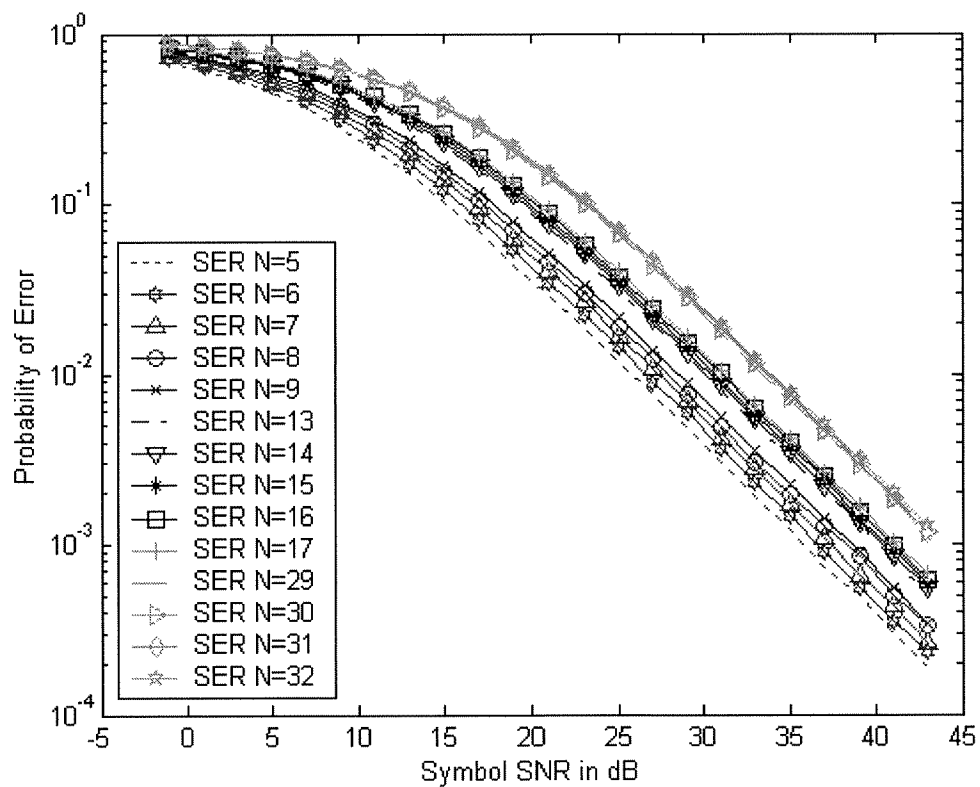
Figure 2.12
SER results for simulation of PAM system
in Rayleigh fading plus AWGN

Figure 2.13 shows the BER performance of the PAM system in Rayleigh

fading plus AWGN. The same trends present in the previous figures are also present

in these BER results. The jump in BER between $N_1 = 8, 9$ and $N_1 = 16, 17$ is even

more evident in this figure.
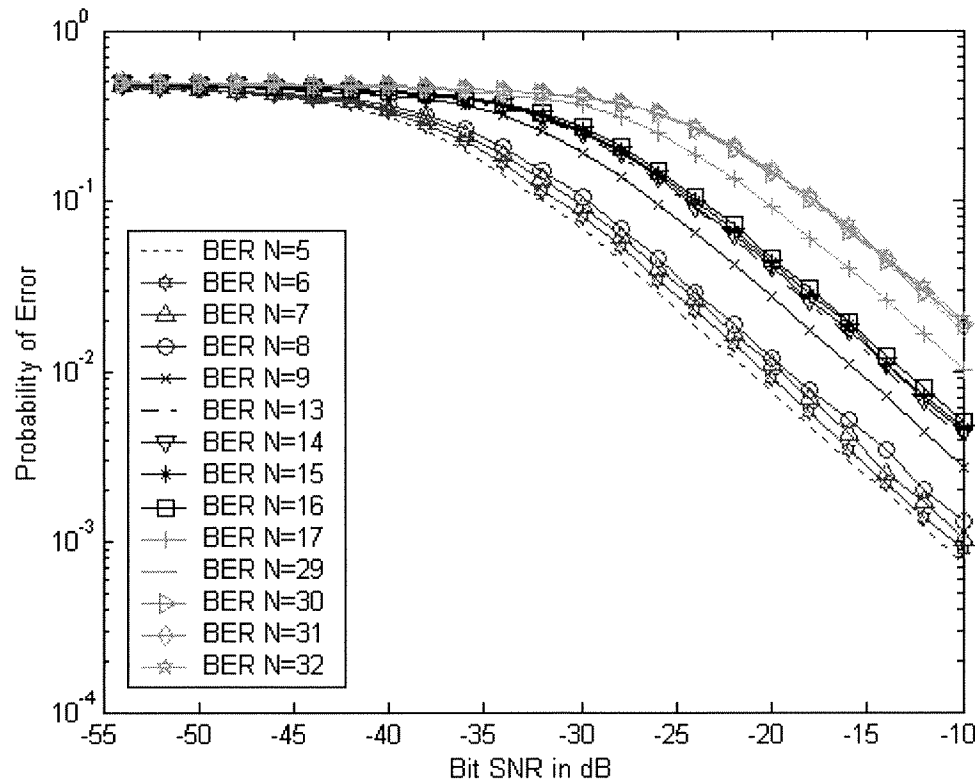
Figure 2.13
BER results for simulation of PAM system
in Rayleigh fading plus AWGN

Figures 2.14 and 2.15 present the improvement in SNR seen between the

different constellations used for simulation. From these figures, it can be seen that the

SNR improvement between the constellations decreases as larger constellations are

used. Note that all possible constellations are not represented in the figures.

	SSNR in dB	dB Separation		BSNR in dB	dB Separation
N1=5	19.703			-32.8093	
		0.9214			0.976
N1=6	20.6244			-31.8333	
		0.6256			0.5
N1=7	21.25			-31.3333	
		0.6833			1.0721
N1=8	21.9333			-30.2612	
		0.2978			0.3862
N1=9	22.2311			-29.875	
		1.511			1.2973
N1=13	23.7421			-28.5777	
		0.6028			0.0833
N1=14	24.3449			-27.75	
		0.1175			0.0833
N1=15	24.4624			-27.6667	
		0.7043			0.8334
N1=16	25.1667			-26.8333	
		0.1024			0.1051
N1=17	25.2691			-26.7282	
		2.2821			2.2926
N1=29	27.5512			-24.4356	
		0.1488			0.1857
N1=30	27.7			-24.2499	
		0.125			0.3336
N1=31	27.825			-23.9163	
		0.1013			0.1666
N1=32	27.9263			-23.7497	
		total = 8.22			total = 9.06

Figure 2.14

The improvement in SNR at a probability of error of 10^{-5},
between constellations produced by the Walsh-code
modulator in an AWGN channel

	SSNR in dB	dB Separation		BSNR in dB	dB Separation
N1=5	25.7182			-21.2783	
		0.7997			0.8154
N1=6	26.5179			-20.4629	
		0.7743			0.86
N1=7	27.2922			-19.6029	
		0.5387			0.4619
N1=8	27.8309			-19.141	
		0.5957			3.5871
N1=9	28.4266			-15.5539	
		1.6148			1.6374
N1=13	30.0414			-13.9165	
		0.2859			0.2632
N1=14	30.3273			-13.6533	
		0.2983			0.2865
N1=15	30.6256			-13.3668	
		0.3883			0.2866
N1=16	31.0139			-13.0802	
		0.1679			3.184
N1=17	31.1818			-9.8962	
		2.255			2.4484
N1=29	33.4368			-7.4478	
		0.2395			0.1969
N1=30	33.6763			-7.2509	
		0.1135			0.0417
N1=31	33.7898			-7.2092	
		0.0785			0.2765
N1=32	33.8683			-6.9327	
		total = 8.15			total = 14.35

Figure 2.15
The improvement in SNR at a probability of error of 10^{-2},
between constellations produced by the Walsh-code
modulator in a Rayleigh fading channel

The results presented above show, that, if the fading experienced in the

channel changes over time, a desired level of error performance is achievable by

switching the constellation used to transmit the signal. This is possible over a 14dB

SNR range for the BER. A simple algorithm is used to switch between constellations

in an effort to maintain a given BER. The algorithm starts by testing the channel by

transmitting a 10^5 bits starting with the largest constellation, where $N_1 = 32$. It tests

until it finds a constellation that gives the desired BER. Then it transmits blocks of

10^6 bits until the BER is found to be too high. Once the BER is found to be too high,

the process is repeated again. Further work could be done to optimize the search

algorithm to determine how often the channel statistics should be returned to the

receiver and how to efficiently switch between constellations based on the expected

magnitude and speed of the fading. Figure 2.16 highlights the scenario of trying to

maintain a BER of 10^{-3} while the fading experienced in the channel fluctuates. The

peaks correspond to the algorithm testing the channel trying to find the constellation

that will give the desired BER. The first peak starts at $N_1 = 32$ and drops down to $N_1 =$

9. The BER can be seen to fluctuate as the channel fluctuates over a large number of

transmitted bits. The second peak drops to $N_1 = 15$ and the third peak drops back to

$N_1 = 9$. The amount of fluctuation in the BER reported across the channel can cause

the algorithm to have to repeat a search multiple times as evident with the second and

third peaks. Since the algorithm always tests from the largest constellation downward,

a more efficient approach would be to switch to the nearest neighbors of the current

constellation if the BER fluctuates.
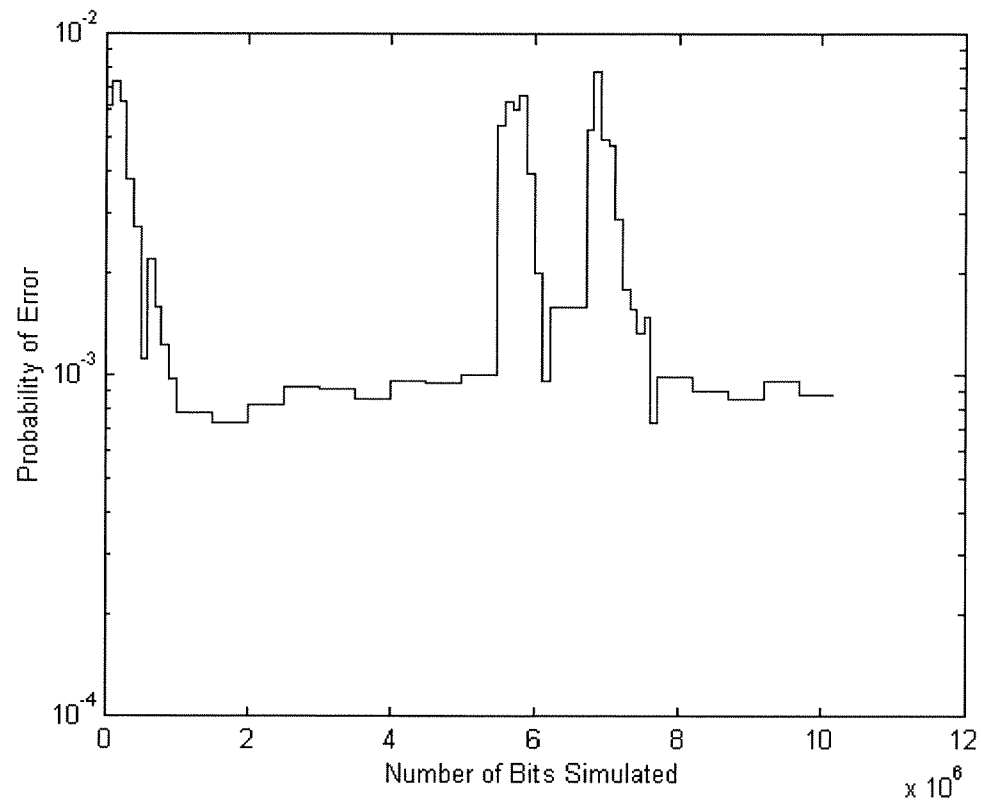
Figure 2.16
System maintains a BER of 10^{-3} as the fading
experienced in the channel fluctuates

Figure 2.17 shows how the number of links available to transmit over,

corresponds to the magnitude of the fading experienced in the channel. As the fading

increases the number of links available decreases.
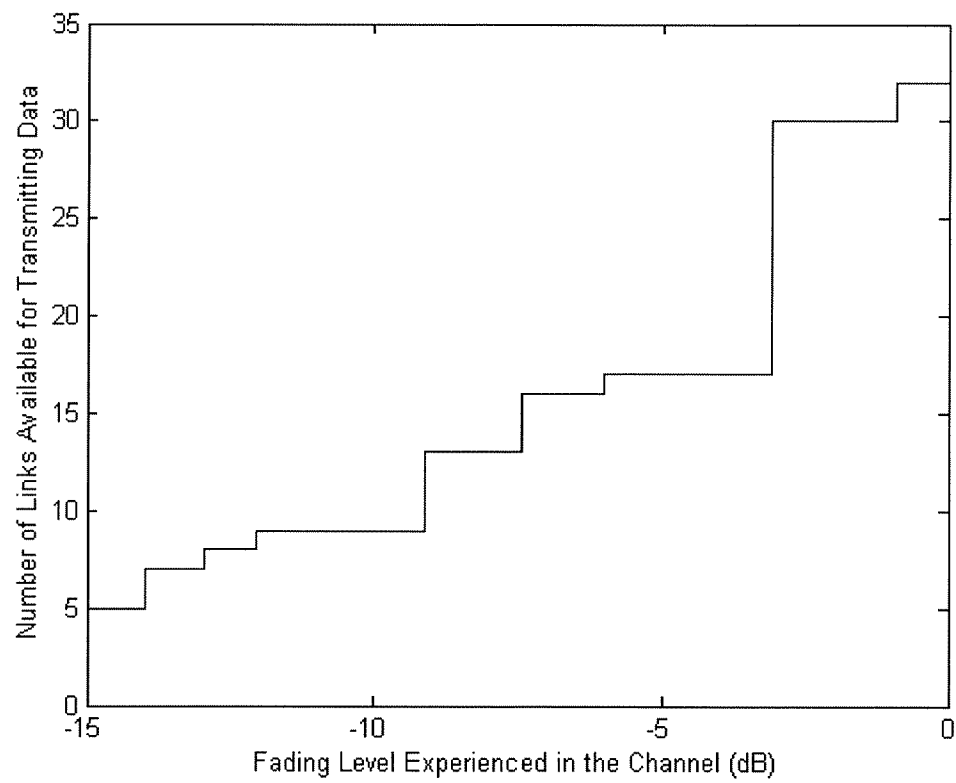
Figure 2.17
Number of links available for transmitting data versus
the level of fading experienced in the channel

3 Walsh-code Modulator with QAM

In an effort to improve the efficiency and performance of the transceiver,

mapping the PAM signal generated by the Walsh-code modulator onto a QAM

constellation was investigated. This modification to the Walsh-code modulator was

successful in improving the symbol error rate performance. The results for the bit

error rate with this simulation showed a similar improvement in error rate. But,

further investigation into the QAM system with the Walsh-code modulator is needed

due to the fact that an increased bit error rate has been seen by other researchers using

similar type systems. This section briefly describes the design methodology for

adding QAM modulation to the Walsh-code modulator.
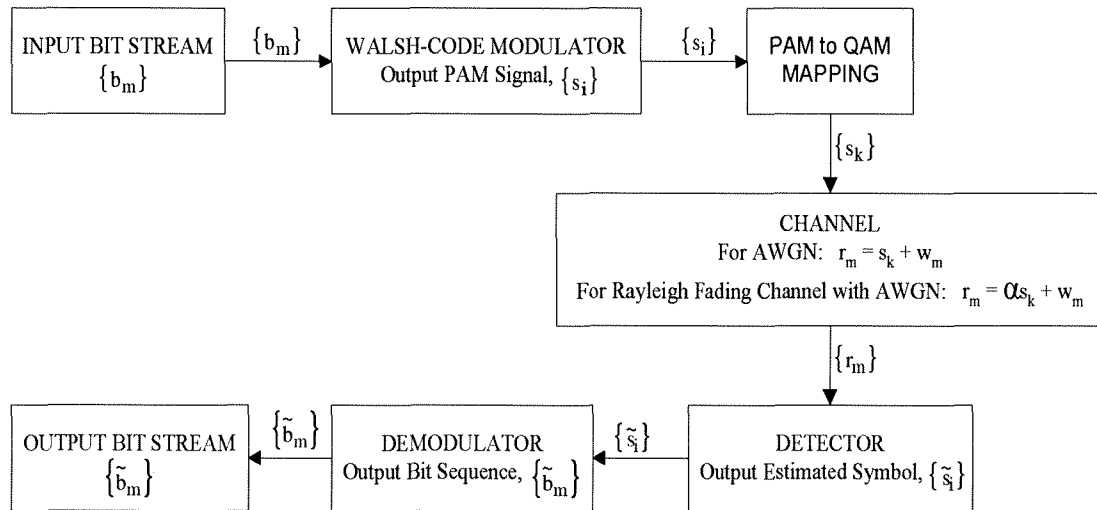
Figure 3.1
QAM system model block diagram

3.1 Choosing a Lattice for Generating a Constellation

Several papers have addressed the problem of how to design a lattice

constellation that has good performance in both AWGN channels and in channels with

fading. To design a lattice with minimum energy and the best performance over a

Rayleigh fading channel, the design methodology presented in Boutros, et al. 1996,

and Giraud, et al. 1996, uses a totally real algebraic number field approach with

minimum absolute discriminant and its reduced minimal polynomial to construct the

lattice based on the criteria presented in those papers. The other approach used in

Boutros, et al. 1996, takes a known good lattice for the AWGN channel and

determines the optimum rotation angle for the lattice to increase its diversity and

maximize its minimum product distance in order to improve its performance over a

Rayleigh fading channel. For the two-dimensional case, the lattice generator matrix

designed for the Rayleigh channel that appears in both papers is shown in equation

3.1.

$$G = \begin{bmatrix} 1 & 1 \\ \dfrac{1}{1+\sqrt{5}} & \dfrac{1}{1-\sqrt{5}} \\ 2 & 2 \end{bmatrix} \tag{3.1}$$

Also, presented in Boutros, et al. 1996, is an optimal square lattice that has been

rotated to improve its performance in the Rayleigh channel. This generator matrix is

shown in equation 3.2.

$$G = \begin{bmatrix} \dfrac{-5+\sqrt{5}}{2} & \dfrac{-5-\sqrt{5}}{2} \\ -\sqrt{5} & \sqrt{5} \end{bmatrix} \tag{3.2}$$

Figure 3.2 shows the performance of these two constellations in AWGN and

figure 3.3 shows their performance in Rayleigh fading plus AWGN. The performance

of a square constellation is included for comparison purposes.
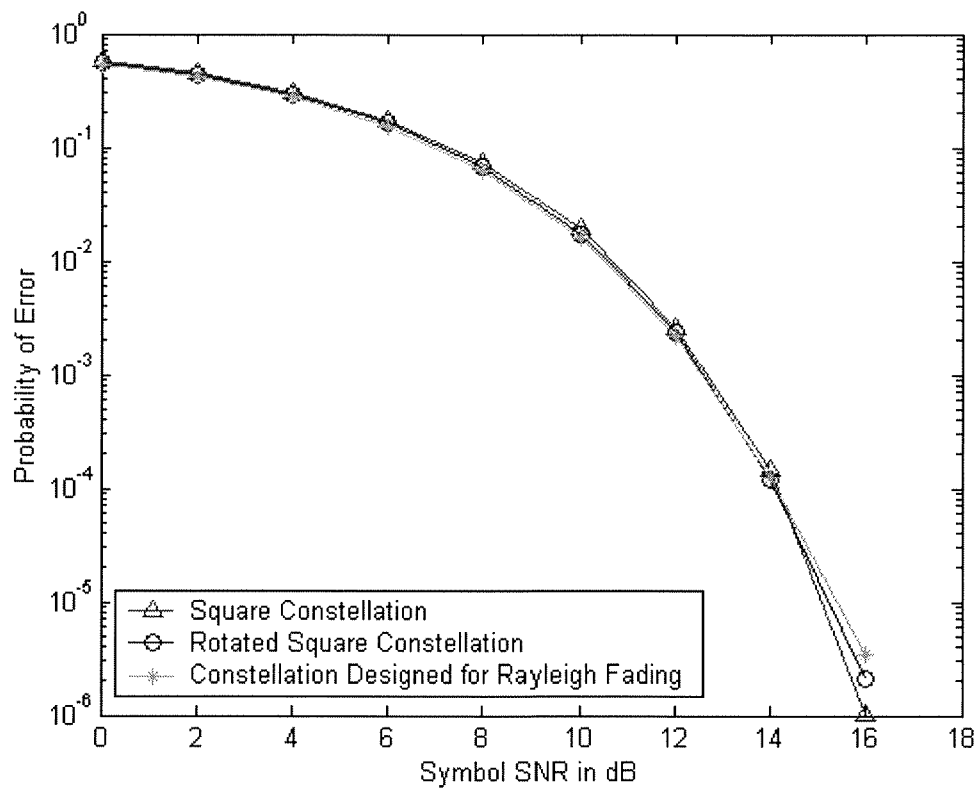
Figure 3.2
Performance of different constellations in AWGN with $N_1=8$
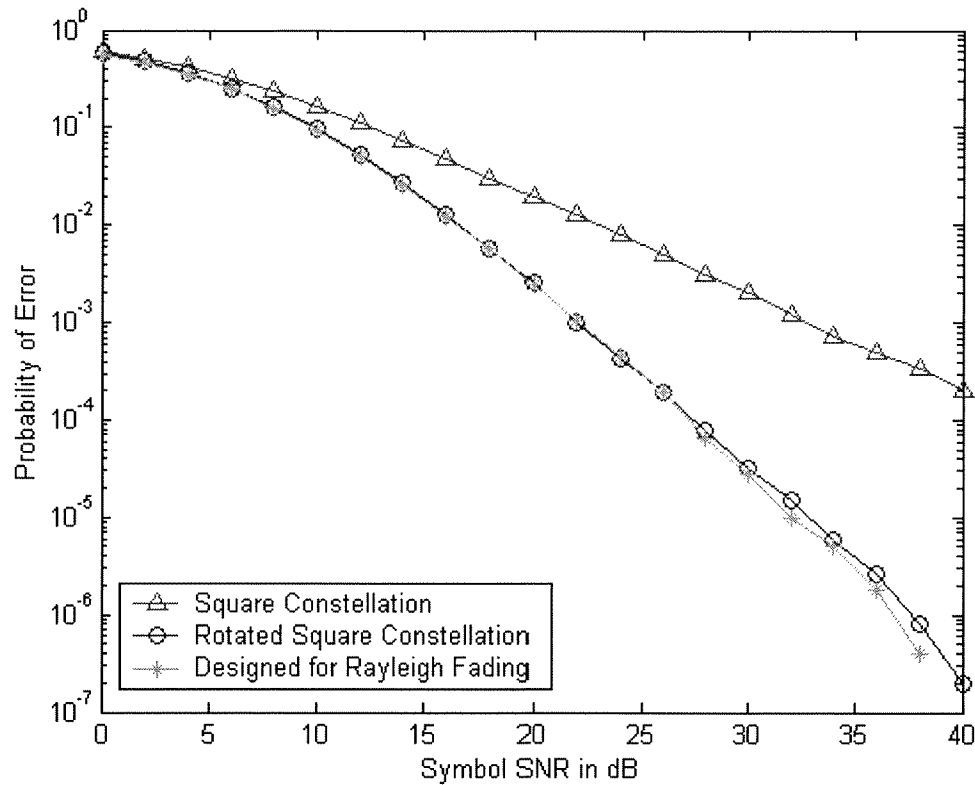
Figure 3.3
Performance of Different Constellations
in Rayleigh fading plus AWGN

The performance of the rotated square lattice and the lattice designed for

Rayleigh fading are very close to each other. In the AWGN channel, the rotated

square lattice shows better performance at a SNR of 16 than the lattice designed for

Rayleigh fading. In the Rayleigh channel with AWGN, the two lattices start to

diverge slightly at the higher SNR. These two trends in the performance of the lattices

are consistent with previous performance reports (Boutros, et al. 1996). The lattice

designed for Rayleigh fading presented in Giraud, et al. 1996, is chosen for the rest of

the work and data gathering in this paper because it is reported by Boutros, et al. 1996, that it has better performance over the Rayleigh fading channel than the rotated square lattice, and as figure 3.3 shows, its performance in the AWGN channel is close to the rotated square lattice.

3.2 Constructing a Constellation from the Chosen Lattice

The QAM constellation is chosen from a lattice described by its generator matrix. This matrix is multiplied by a set of integers, thus generating the points of the lattice. To construct a constellation with a specific number of points, choose a set of integers and multiply all linear combinations of this set by the generator matrix. If the number of constellation points is more than the required number, eliminate points based on their distance from the origin and remove them in pairs reflected across the origin. The generator matrix for the lattice that has been designed for Rayleigh fading, and the set of integers used to construct the constellation are shown below (Giraud, et al. 1996).

$$G = \begin{bmatrix} 1 & 1 \\ \dfrac{1+\sqrt{5}}{2} & \dfrac{1-\sqrt{5}}{2} \end{bmatrix} \qquad (3.3)$$

$$i = \begin{bmatrix} 0 & \pm 1 & \pm 2 & \pm 3 \end{bmatrix} \qquad (3.4)$$

The generated lattice and a subset of constellation points are shown in figure

3.4.

Figure 3.4
33 point constellation within the generated 49 point lattice

3.3   Procedure for Mapping the PAM Constellation onto the QAM Constellation

The method used to map the PAM constellation onto the QAM constellation

assigns the PAM symbols most likely to occur to the points of the QAM constellation

with the lowest energy. This method is the first criteria listed by Takahara, et al. 2003, in order to minimize the SER. As expected, this minimum energy assignment method produced the best results in terms of symbol error rate performance, since the effects of the fading and additive noise are minimized. Other assignments, such as assigning the most likely symbols to the highest energy points of the constellation and variations on these two methods, produced results with higher symbol error rates. Figures 3.5 and 3.6, show the performance of different PAM to QAM constellation assignments in AWGN and Rayleigh fading plus AWGN. Further investigation into the assignment of the PAM signal to a QAM constellation is necessary to resolve an issue around these results. At first, the intuitive approach to the assignment procedure would seem suggest that in order to have fewer symbol errors, the highest probability PAM levels should be assigned to the highest energy points of the QAM constellation. The criteria presented by Takahara, et al. 2003, and the simulation results contradict this intuitive approach. Further investigation is needed to resolve why this occurs and to ensure that the simulation results are accurate.
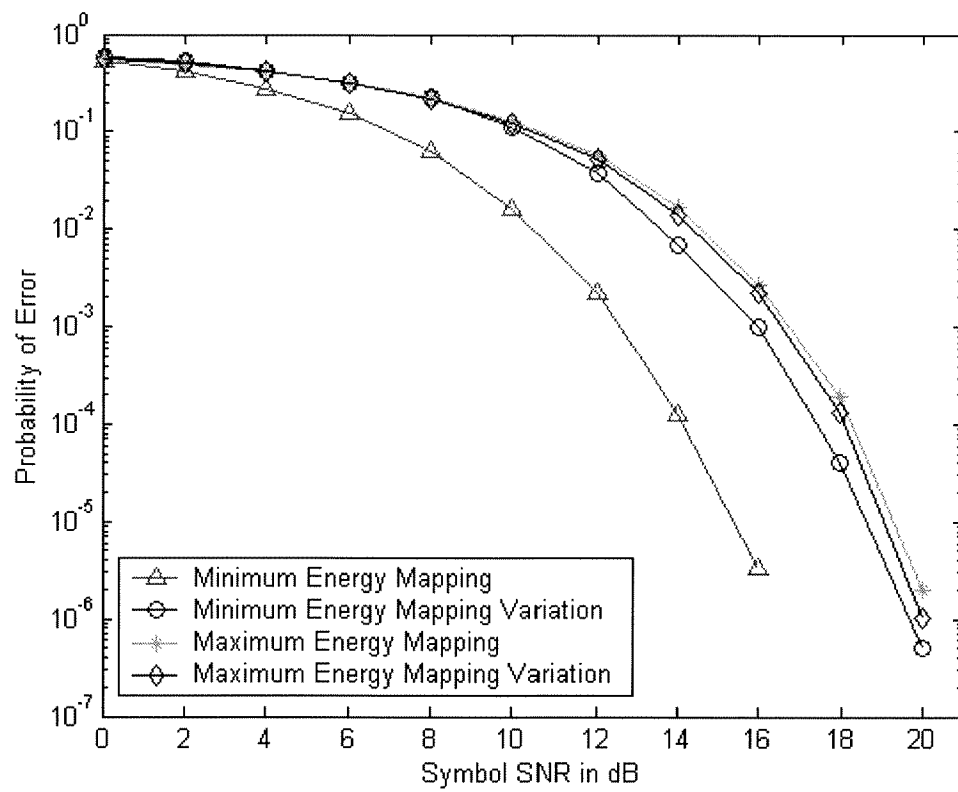
Figure 3.5
Comparison of SER for different mappings of PAM constellation
to QAM constellation in AWGN with $N_1 = 8$
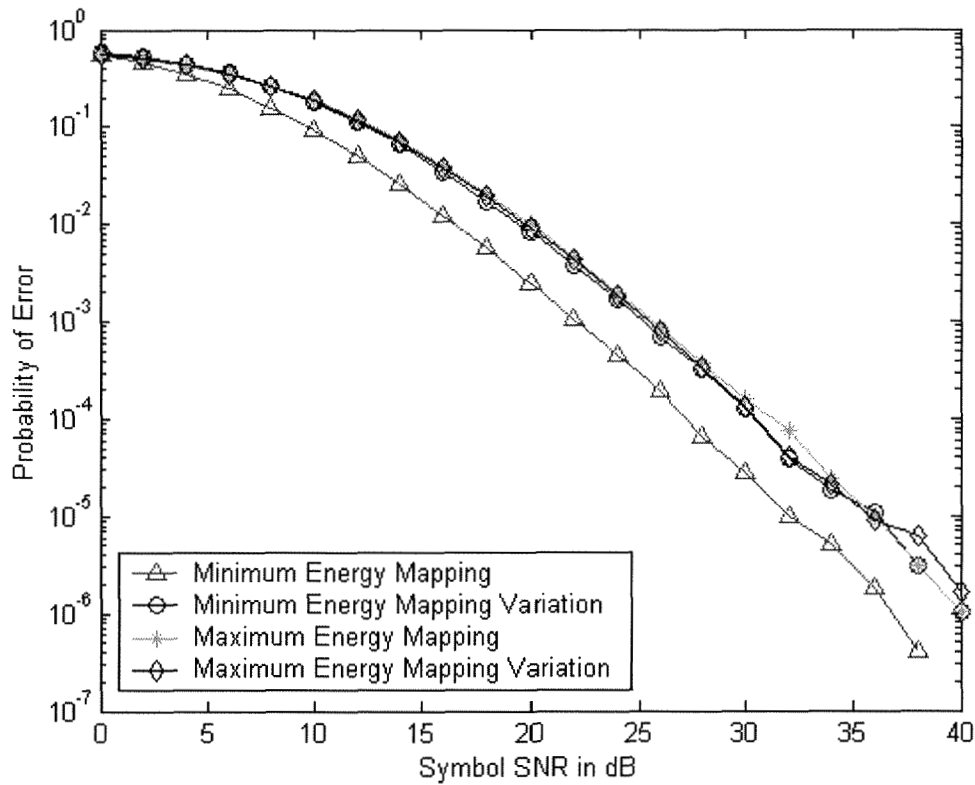
Figure 3.6
Comparison of SER for different mappings of PAM constellation
to QAM constellation in Rayleigh fading plus AWGN for $N_1 = 8$

3.4 Simulation Setup

The simulation setup used for the QAM system is an extension of the

PAM system into two dimensions. The two-dimensional QAM signal is made up of

an inphase and quadrature component. This system contains the same blocks as the

PAM system with the addition of mapping the PAM signal onto a QAM constellation.

Also, a baseband equivalent system model is used to represent the bandpass QAM

system. Therefore, the representation of the noise present in the channel is changed to reflect the difference between the baseband equivalent model and the strict baseband model used for the PAM system. The AWGN is made up of independent inphase and quadrature components that are each applied independently to the inphase and quadrature components of the QAM signal as shown in the following equations.

$$r_{inphase} = s_{inphase} + w_{inphase} \qquad (3.5)$$

$$r_{quadrature} = s_{quadrature} + w_{quadrature} \qquad (3.6)$$

Each of the components has zero mean and variance N_0, due to the double-sided representation of the noise process and the bandpass QAM signal. The Rayleigh fading coefficients are also made up of inphase and quadrature components, that are applied independently to the inphase and quadrature components, shown in equations 3.7 and 3.8.

$$r_{inphase} = \alpha_{inphase} s_{inphase} + w_{inphase} \qquad (3.7)$$

$$r_{quadrature} = \alpha_{quadrature} s_{quadrature} + w_{quadrature} \qquad (3.8)$$

Further, each the inphase and quadrature components have the same characteristics as the coefficients described in the PAM system. The assumptions applied to the baseband PAM system also apply to this QAM system.

3.5   Comparison of the PAM Signal versus the QAM Signal

Mapping the PAM signal generated by the Walsh-code modulator onto a QAM constellation improves the efficiency and performance of the transmitted signal. Figures 3.7 through 3.10 are examples of the improvement in error rate made possible by using the QAM system. When $N_1 = 8$, the improvement in SNR when transmitting through an AWGN channel is approximately 7 dB at a SER and BER of 10^{-5}. When $N_1 = 8$, the improvement in SNR when transmitting through a Rayleigh fading plus AWGN channel is approximately 17 dB at a SER and BER of 10^{-3}.
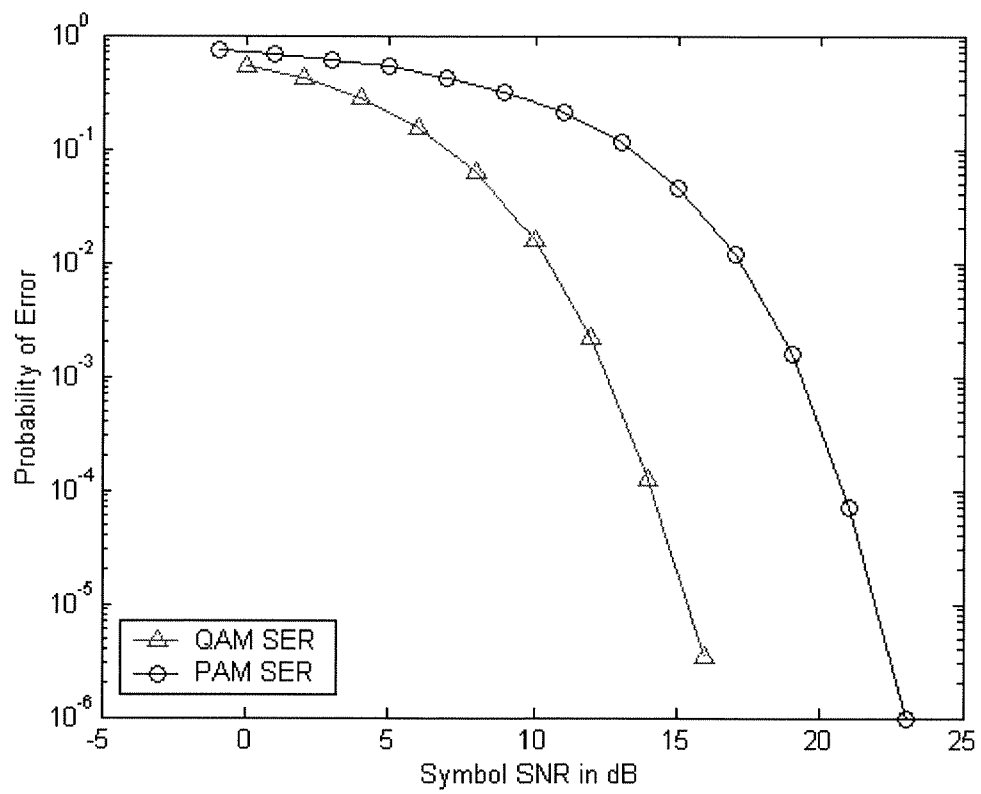
Figure 3.7
Comparison of PAM and QAM SER
performance in AWGN with $N_1 = 8$
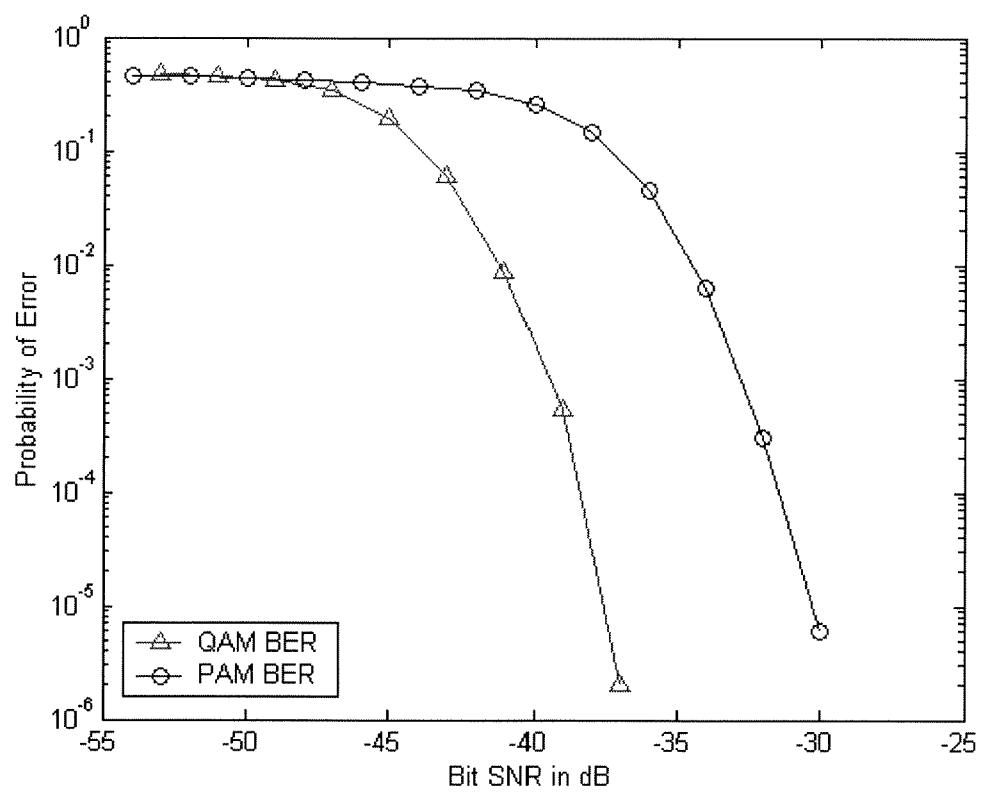
Figure 3.8
Comparison of PAM and QAM BER
performance in AWGN with $N_1 = 8$
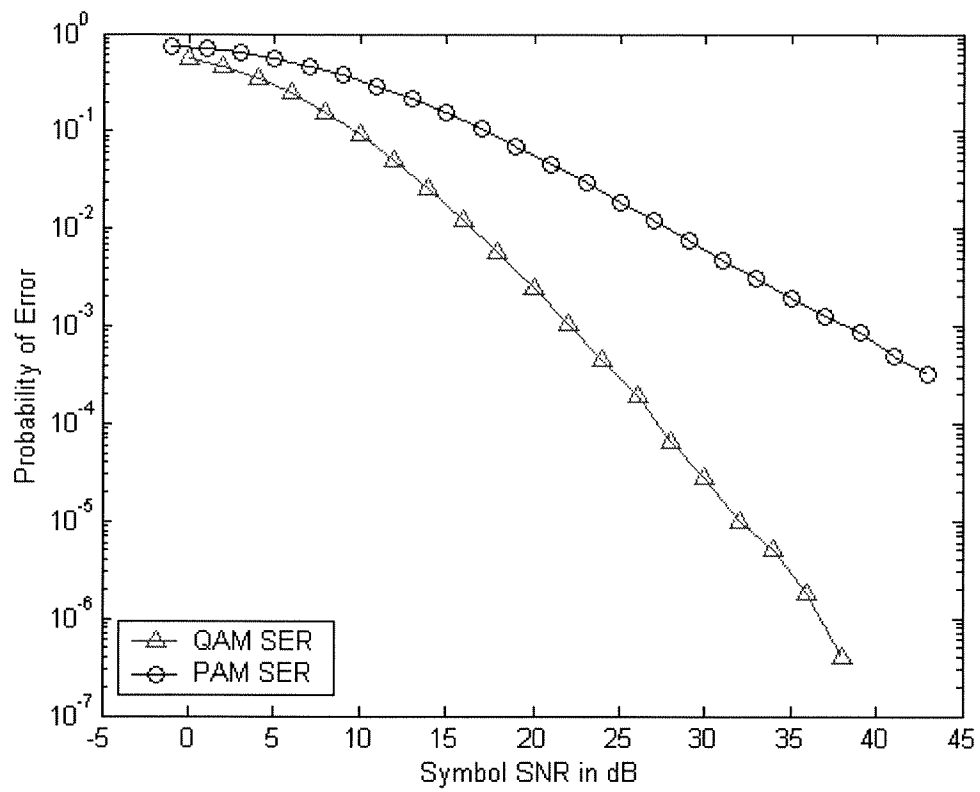
Figure 3.9
Comparison of PAM and QAM SER performance
in Rayleigh fading plus AWGN for $N_1 = 8$
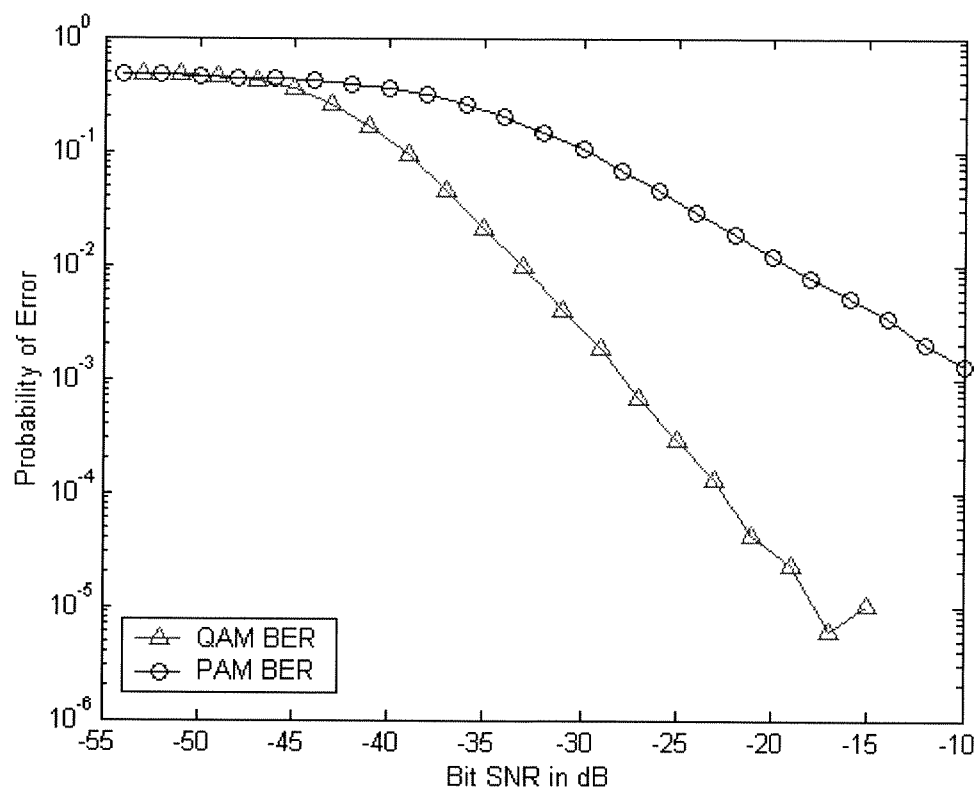
Figure 3.10
Comparison of PAM and QAM BER performance
in Rayleigh fading plus AWGN for $N_1 = 8$

4 Conclusion

Presented in this thesis is a transceiver using a Walsh-code modulator that gives a communication system the ability to adjust its transmitted signal in order to maintain a desired level of error rate performance over a varying channel. This is achieved by using a dynamic demultiplexer and orthogonal codes to separate the input bit stream into sub-streams, which are spread and summed together, producing a variable PAM constellation. The system can achieve a constant BER within a 14dB SNR range in a Rayleigh fading plus AWGN channel. Also, a feature of using demultiplexed sub-streams is that a sequence used to estimate the conditions of the channel can included along with the transmitted data easily. It is also shown that mapping the PAM signal onto a QAM constellation is a way to improve the performance of the overall system. The use of the QAM system was investigated but was not incorporated into the transceiver due to issues that need further investigation to be resolved, to ensure that accurate results and performance are obtained.

BIBLIOGRAPHY

E. Armanious, D. D. Falconer, and H. Yanikomeroglu, "Adaptive Modulation, Adaptive Coding, and Power Control for Fixed Cellular Broadband Wireless Systems: Some New Insights," Submitted to *IEEE WCNC* 2003.

M. Alouini, X. Tang, and A. J. Goldsmith, "An Adaptive Modulation Scheme for Simultaneous Voice and Data Transmission over Fading Channels," *IEEE Journal on Selected Areas in Communications*, vol. 17, no. 5, pp. 837-850, May 1999.

J. Boutros, E. Viterbo, C. Rastello, and J. C. Belfiore, "Good Lattice Constellations for Both Rayleigh Fading and Gaussian Channels," *IEEE Transactions on Information Theory*, vol. 42, no. 2, pp. 502-518, March 1996.

L. W. Couch, *Digital and Analog Communication Systems*, 4th ed., Macmillan, 1993.

X. Giraud and J. C. Belfiore, "Constellations Matched to the Rayleigh Fading Channel," *IEEE Transactions on Information Theory*, vol. 42, no.1, pp. 106-115, January 1996.

A. J. Goldsmith and S. Chua, "Adaptive Coded Modulation for Fading Channels," *IEEE Transactions on Communications*, vol. 46, no. 5, pp. 595-602, May 1998.

A. J. Goldsmith and S. Chua, "Variable-Rate Variable-Power MQAM for Fading Channels," *IEEE Transactions on Communications*, vol. 45, no. 10, pp. 1218-1230, October 1997.

S. Haykin, *Digital Communications*, John Wiley and Sons, 1988.

P. Hoeher and F. Tufvesson, "Channel Estimation with Superimposed Pilot Sequence," *Global Telecommunications Conference 1999, GLOBECOM '99*, vol. 4, pp. 2162-2166.

M. S. Roden, *Analog and Digital Communication Systems*, 4th ed., Prentice Hall, 1996

M. Schwartz, *Information Transmission, Modulation, and Noise*, 3rd ed., McGraw-Hill, 1980.

BIBLIOGRAPHY (Continued)

F. G. Stremler, *Introduction to Communication Systems*, 3rd ed., Addison-Wesley, 1990.

G. Takahara, F. Alajaji, N. C. Beaulieu, and H. Kuai, "Constellation Mappings for Two-Dimensional Signaling of Nonuniform Sources," *IEEE Transactions on Communications*, vol. 51, no. 3, pp. 400-408, March 2003.

J. M. Torrance and L. Hanzo, "Performance Upper Bound of Adaptive QAM in Slow Rayleigh Fading Environments," *ISPACS '96 Singapore 26-28 November 1996*, pp. 1652-1657.

E. Viterbo and J. Boutros, "A Universal Lattice Code Decoder for Fading Channels," *IEEE Transactions on Information Theory*, vol. 45, no. 5, pp. 1639-1642, July 1999.

W. T. Webb and R. Steele, "Variable Rate QAM for Mobile Radio," *IEEE Transactions on Communications*, vol.43, no. 7, pp. 2223-2230, July 1995.

APPENDICES

A   PAM Simulation System Description

A.1   System Assumptions

For simulation, the PAM system is modeled as a baseband system. The following assumptions are made about the system. The transmitted waveform consists of rectangular pulses. The bit rate (R_b) = 100kbps. There is coherent reception with perfect phase estimation, synchronization, and sampling of the received signal at the detector. A feedback channel from the receiver to the transmitter is available, providing the transmitter with accurate channel characterization and error performance information about the received signal. Also, the bit signal-to-noise ratio is defined as $\frac{E_b}{N_0}$ and the symbol signal-to-noise ratio is defined as $\frac{2E_{av}}{N_0}$.
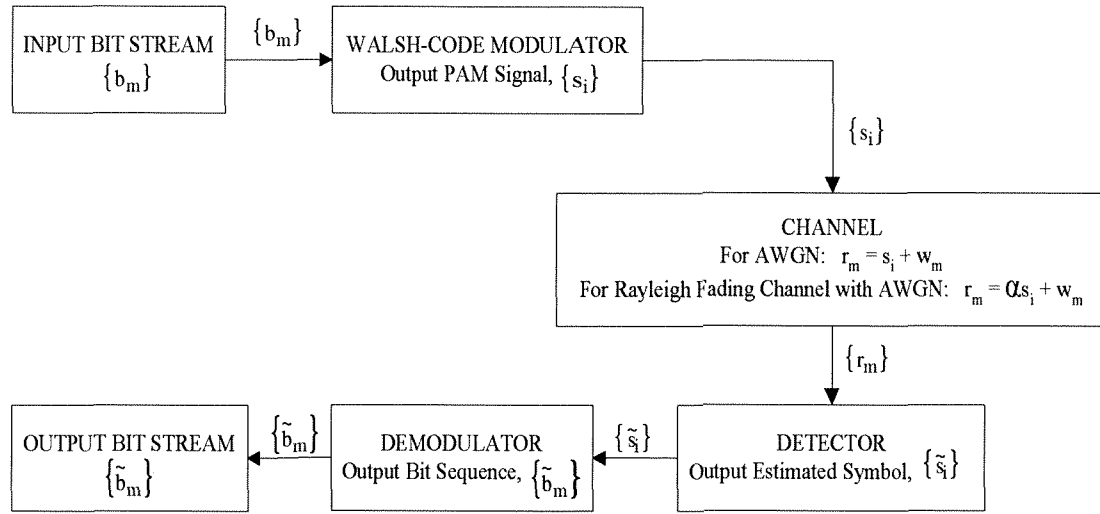
Figure A.1
PAM system model block diagram

A.2 Description of System Input

The input to the system consists of binary data in the form of either a "1" or a "0". The input bits occur with equal probability and have a uniform distribution.

A.3 Description of the Walsh-code Modulator

The Walsh-code modulator takes the input bit stream and transforms it into a multi-level PAM signal through the following operations. First, the input bit stream is demultiplexed into N_1 sub-streams. After this has occurred, the sub-streams are converted into a polar representation where an input "1" is converted to a value of +1

and an input "0" is converted into a value of -1. This is done in order to utilize the orthogonal properties of the Walsh-Hadamard matrix used in the next operation. A Walsh-Hadamard matrix is a matrix where all of its rows are orthogonal to each other. In order to be orthogonal to each other, the values of the column entries in these rows consist of either a 1 or a -1. The Walsh-Hadamard matrix is generated so that the length of each orthogonal row is equal to or greater than the number of demultiplexed sub-streams. An example of the generation of Walsh-Hadamard matrices is provided in figure A.2.

$$H_1 = [1]$$

$$\overline{H}_1 = [-1]$$

$$H_2 = \begin{bmatrix} H_1 & H_1 \\ H_1 & \overline{H}_1 \end{bmatrix} = \begin{bmatrix} 1 & 1 \\ 1 & -1 \end{bmatrix}$$

$$\overline{H}_2 = \begin{bmatrix} -1 & -1 \\ -1 & 1 \end{bmatrix}$$

$$H_4 = \begin{bmatrix} H_2 & H_2 \\ H_2 & \overline{H}_2 \end{bmatrix} = \begin{bmatrix} 1 & 1 & 1 & 1 \\ 1 & -1 & 1 & -1 \\ 1 & 1 & -1 & -1 \\ 1 & -1 & -1 & 1 \end{bmatrix}$$

Figure A.2
Generation of Walsh-Hadamard matrices by recursion

The Walsh-Hadamard matrix is used to spread the demultiplexed sub-streams. This is performed by multiplying each of the demultiplexed sub-streams by one row of a Walsh-Hadamard matrix. Figure A.3 shows this spreading procedure.

$$\text{Input bit sequence} = \begin{bmatrix} 1 & -1 & 1 & -1 \end{bmatrix}$$

$$\text{Demultiplexed sub-streams} = \begin{bmatrix} 1 \\ -1 \\ 1 \\ -1 \end{bmatrix}$$

$$\text{Walsh-Hadamard codes} = \begin{bmatrix} 1 & 1 & 1 & 1 \\ 1 & -1 & 1 & -1 \\ 1 & 1 & -1 & -1 \\ 1 & -1 & -1 & 1 \end{bmatrix}$$

$$\text{Spread sub-streams} = \begin{bmatrix} 1 & 1 & 1 & 1 \\ -1 & 1 & -1 & 1 \\ 1 & 1 & -1 & -1 \\ -1 & 1 & 1 & -1 \end{bmatrix}$$

Figure A.3
Spreading procedure with $N_1 = 4$

The purpose of the spreading operation is to create a number of independent, or orthogonal, links for the data to be transmitted over and to spread the spectrum of the demultiplexed sub-streams. After demultiplexing and spreading, the resulting orthogonal streams are summed together on a chip-by-chip basis before transmission. Figure A.4 shows this summing operation.

$$\text{Spread sub-streams} = \begin{bmatrix} 1 & 1 & 1 & 1 \\ -1 & 1 & -1 & 1 \\ 1 & 1 & -1 & -1 \\ -1 & 1 & 1 & -1 \end{bmatrix}$$

$$\text{Summed output} = \begin{bmatrix} 0 & 4 & 0 & 0 \end{bmatrix}$$

Figure A.4
Walsh-code modulator sub-stream summing operation

The result of the summing operation is a multi-level output signal from the Walsh-code modulator. This PAM signal has N_1+1 levels and a symbol rate that is equal to or greater than the original input bit rate. For example, when $N_1=7$ the number of PAM levels produced is 8, and when $N_1=8$ the number of PAM levels produced is 9. Therefore, when N_1 is even, the number of PAM levels produced is odd, including the 0 level. When N_1 is odd, the number of PAM levels is even, excluding the 0 level. The levels in the PAM constellation produced by the Walsh-code modulator occur with a Gaussian-like probability distribution centered at zero, as shown in figure A.6. The Walsh-code modulator uses Walsh-Hadamard codes of length $N_2 = 8$, 16, or 32. This means that the number of demultiplexed sub-streams can vary from 5-8 when using the length 8 codes, from 9-16 when using the length 16 codes, and from 17-32 when using the length 32 codes. When the value of N_1 is equal to the length of the orthogonal code, the output symbol rate (R_c) is equal to the input bit rate (R_b). When the number of demultiplexed sub-streams is less than the length of the orthogonal code, the symbol, or chip rate, is proportional to the input bit rate

described by: $R_c = (N_2*R_b)/N_1$. For $N_1 = 8$, 16, or 32 the PAM output symbol rate is

equal to the input bit rate. For $N_1 < 8$, 16, or 32 the output symbol rate is higher than

the input bit rate. For example if $N_1 = 7$, $R_c = (8*100\text{kbps})/7$ 114kbps, 14% higher.

A block diagram of the Walsh-code modulator is found in figure A.5.

Figure A.5
Walsh-code modulator
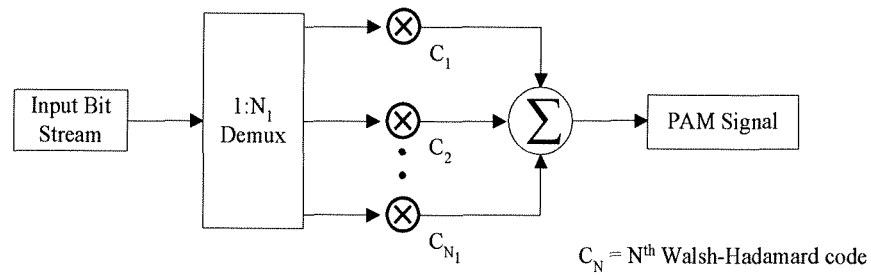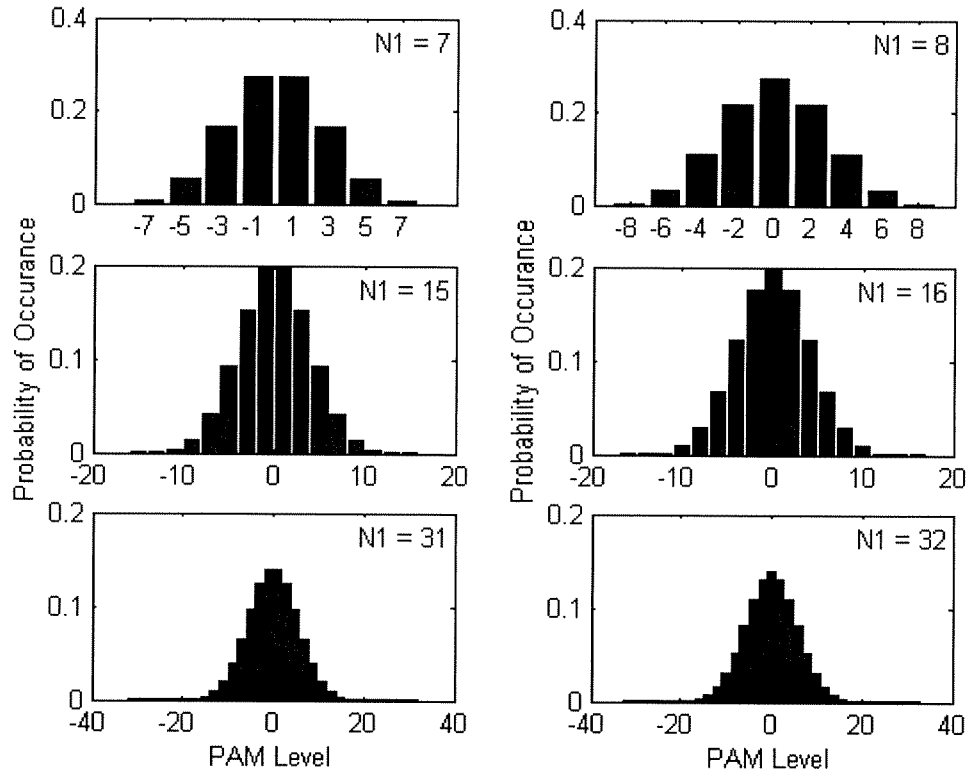
Figure A.6
Histograms of distribution of PAM levels
produced with N_1 = 7, 8, 15, 16, 31, 32

A.4 Description of the Channel

In the baseband model used for simulation of the PAM system, the AWGN

present in the channel is modeled as a white noise process with power spectral density

(N_0), having a Gaussian distribution with zero mean and variance $\dfrac{N_0}{2}$. N_0 has a value

of 10^{-11}. Therefore, the received signal (r) consists of the transmitted signal plus the noise (w), represented in equation A.1.

$$r_m = s_i + w_m \qquad \text{(A.1)}$$

The Rayleigh fading channel is modeled with independent fading coefficients, which are a multiplicative component (α) applied to the transmitted signal as shown in the following equation.

$$r_m = \alpha s_i + w_m \qquad \text{(A.2)}$$

The fading coefficients have a Rayleigh distribution and are characterized by the following equations.

$$f(\alpha) = \frac{\alpha}{\sigma^2} e^{\left(\frac{\alpha^2}{2\sigma^2}\right)} \qquad \text{(A.3)}$$

$$E\{\alpha\} = \sqrt{\frac{\pi}{2}}\sigma \qquad \text{(A.4)}$$

$$E\{\alpha^2\} = 2\sigma^2 \qquad \text{(A.5)}$$

The fading coefficients are normalized, so that $E\{\alpha\} = 1$, therefore, $\sigma = \sqrt{\frac{2}{\pi}}$.

The fading coefficients are generated using two Gaussian random variables (x, y) with variance σ^2. The generation of α is shown below (Roden 1996).

$$\alpha = \sqrt{x^2 + y^2} \qquad \text{(A.6)}$$

A.5   Relationship of the Bit Energy to the Transmitted Symbol Energy

During simulation, the data is operated on in a block by block manner, and as a result, time is not explicit during the simulation. In order to maintain the proper relationship between the input bit energy and the transmitted symbol energy, the introduction of a scaling factor applied to the signal before transmission is necessary. The following figures and equations provide the basis for determining the correct value of this scaling factor.

The following equation represents the input bit stream.

$$b_n(t) = \sum_{n=-\infty}^{\infty} A_n b_n(t - nT_b) \qquad (A.7)$$
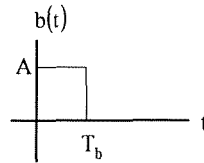
Figure A.7
Graphical representation of the input bit stream

Given the value of N_0, the bit energy (E_b) required to give a desired signal-to-noise ratio (SNR) can be determined in the following equations.

$$SNR = 10\log_{10} \frac{E_b}{N_0} \qquad (A.8)$$

$$E_b = N_0 10^{\left(\frac{SNR}{10}\right)} \qquad (A.9)$$

Given the value of T_b, the amplitude (A) necessary to give the desired E_b can be found by the following procedure.

$$E_b = A^2 T_b \qquad (A.10)$$

$$A = \pm \sqrt{\frac{E_b}{T_b}} \qquad (A.11)$$

At the first stage in the Walsh-code modulator the input bits are demultiplexed into N_1 sub-streams. The amplitude of the bits is unchanged after passing through the demultiplexer. The representation of the demultiplexed bits is found in equation A.12 and figure A.8. The calculation of the energy present in each demultiplexed bit is found in equation A.13.

$$\overline{b}_{nj}(t) = \sum_{n=-\infty}^{\infty} A_n \overline{b}_n (t - nN_1 T_b) \qquad j = 1,2,...,N_1 \qquad (A.12)$$

$$E_d = A^2 N_1 T_b \qquad (A.13)$$
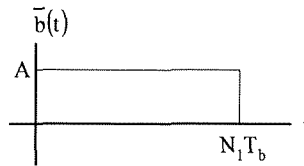
Figure A.8
Graphical representation of the demultiplexed sub-streams

At the second stage in the Walsh-code modulator, the demultiplexed sub-streams are spread using Walsh-Hadamard codes. The amplitude of the chips in the spreading code are normalized to have values of ± 1, so that the amplitude of the resulting spread signal is not amplified. The number of chips in the spreading code (c_j) is N_2. The representation of the spread chips is found in equation A.14. The representation of the spread sub-streams is found in equation A.16. The energy present in each chip is found in equation A.17.

$$\hat{b}_{c_{ij}}(t) = \sum_{i=1}^{N_2} A_i \hat{b}_{c_j}\left(t - i\left(N_1 T_b / N_2\right)\right) \qquad j = 1,2,\ldots,N_1 \qquad (A.14)$$

$$\hat{b}_{nj}(t) = \sum_{n=-\infty}^{\infty} A_n \bar{b}_n \left(t - n N_1 T_b\right) \otimes c_j \qquad\qquad (A.15)$$

$$\hat{b}_{nj}(t) = \sum_{n=-\infty}^{\infty} \sum_{i=1}^{N_2} A_n \hat{b}_{c_j}\left(t - n N_1 T_b - i\left(N_1 T_b / N_2\right)\right) \qquad (A.16)$$

$$E_c = \frac{A^2 N_1 T_b}{N_2} \qquad\qquad (A.17)$$
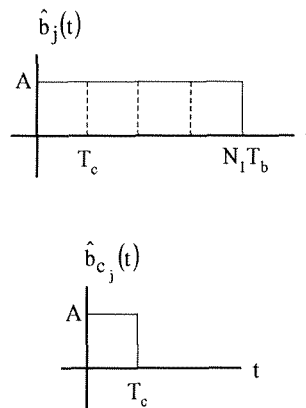
Figure A.9
Graphical representation of the spread sub-stream

Summing the spread sub-streams over each chip interval is the final operation

in the Walsh-code modulator. This operation produces the multi-level PAM signal

with symbols (s_n) having a duration equal to the chip duration of

$$T_c = N_1 T_b / N_2 \qquad (A.18)$$

The output PAM symbols are represented by equation A.19.

$$s_n(t) = \sum_{n=-\infty}^{\infty} \sum_{i=1}^{N_2} \sum_{j=1}^{N_1} A_n \hat{b}_{c_j} \left(t - nN_1 T_b - i(N_1 T_b / N_2) \right) \qquad (A.19)$$

Using the description for the PAM constellation presented in appendix B, the

levels of the constellation are separated by a certain distance (d). This is the scaling

factor that should be used to scale the constellation to the correct average energy for a

given input bit energy. Using the representation of the PAM constellation in figure

A.10, where d is explicitly shown, the average energy (E_{av}) of the constellation is

found by equation A.20.

$$E_{av} = \sum_{i=1}^{M} s_i{}^2 P\{s_i\} \qquad\qquad (A.20)$$

i = 1   2   · · ·   -4d -3d -2d -d   0   d   2d   3d   4d   · · ·   M-1   M s_i

$\dfrac{-(M-1)d}{2}$ $\qquad\qquad\qquad\qquad\qquad\qquad\qquad\qquad\qquad\qquad\qquad$ $\dfrac{(M-1)d}{2}$
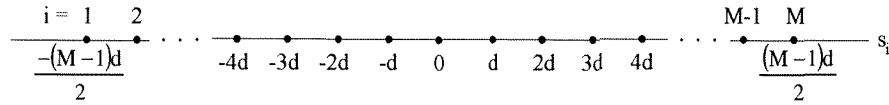
Figure A.10
Graphical representation of the PAM constellation
produced when N_1 is even valued

i = 1   2   · · · $\dfrac{-7d}{2}$ $\dfrac{-5d}{2}$ $\dfrac{-3d}{2}$ $\dfrac{-d}{2}$ $\dfrac{d}{2}$ $\dfrac{3d}{2}$ $\dfrac{5d}{2}$ $\dfrac{7d}{2}$ · · ·   M-1   M s_i

$\dfrac{-(M-1)d}{2}$ $\qquad\qquad\qquad\qquad\qquad\qquad\qquad\qquad\qquad\qquad\qquad$ $\dfrac{(M-1)d}{2}$
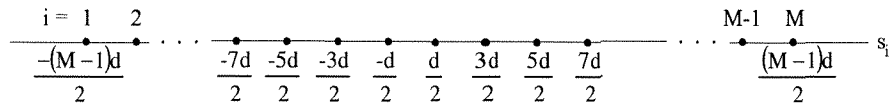
Figure A.11
Graphical representation of the PAM constellation
produced when N_1 is odd valued

For any constellation, the energy in the maximum energy level present in the constellation is equal to E_c*N_1. It is possible to find the value of d by using the first constellation symbol (s_1), which has the maximum energy. The calculation of the value of d is shown in the following equations.

$$E_{s_1} = s_1{}^2 T_c = (L_1 d)^2 T_c = E_c N_1 \qquad\qquad (A.21)$$

$$d = \frac{\sqrt{\dfrac{E_c N_1}{T_c}}}{L_1} \qquad\qquad (A.22)$$

After the scaling factor has been determined it must be applied to the PAM

signal before transmission. In simulation, the PAM signal is generated using integer

values, so the PAM signal will also have integer values. This means that a

relationship between the generated integer constellation, and the constellation used to

determine the scaling factor must be found, in order to determine the final scaling

factor applied to the generated PAM signal. By relating the two constellations, the

final scaling factor turns out to be equal to $\dfrac{d}{2}$.

A.6   Detection of the Received PAM Signal

At the receiver, maximum-likelihood symbol detection is performed using a

minimum Euclidean distance metric that determines which constellation point the

received signal is closest to. Equation A.23 shows the metric used (Haykin 1988;

Boutros, et al. 1996).

$$d = \left\| r_m - s_i \right\|^2 \qquad\qquad (A.23)$$

For the case of an AWGN channel, to recover the originally transmitted signal,

the received symbols are compared to the constellation used to transmit the signal, and

the constellation point closest to the received symbol is declared to be the transmitted

symbol. Similarly, for the case of a Rayleigh fading plus AWGN channel, to recover

the original signal, each received symbol is compared to the constellation used to

transmit the signal after it has been compressed by the fading channel coefficient corresponding to the interval for that received symbol. Once again, the constellation point closest to the received symbol is declared to be the transmitted symbol (Boutros, et al. 1996; Viterbo, et al. 1999).

After the transmitted symbol has been determined, demodulation of the received symbols for bit recovery takes place. Demodulation is performed by despreading a block of N_2 received symbols using the same orthogonal codes used to spread the original bit streams. To recover the transmitted bit sequence, the block of N_2 symbols is multiplied by each Walsh-Hadamard code used to spread the signal, and then divided by the length of the Walsh-Hadamard code. Figure A.12 shows the demodulation procedure.

$$r_m = \begin{bmatrix} 0 & 4 & 0 & 0 \end{bmatrix}$$

$$\text{Walsh-Hadamard codes (W\_H)} = \begin{bmatrix} 1 & 1 & 1 & 1 \\ 1 & -1 & 1 & -1 \\ 1 & 1 & -1 & -1 \\ 1 & -1 & -1 & 1 \end{bmatrix}$$

bit sequence = $(r_m * W\_H)/4$

$$r_m * W\_H = \begin{bmatrix} 0 & 4 & 0 & 0 \end{bmatrix} * \begin{bmatrix} 1 & 1 & 1 & 1 \\ 1 & -1 & 1 & -1 \\ 1 & 1 & -1 & -1 \\ 1 & -1 & -1 & 1 \end{bmatrix} = \begin{bmatrix} 4 & -4 & 4 & -4 \end{bmatrix}$$

bit sequence $= \begin{bmatrix} 4 & -4 & 4 & -4 \end{bmatrix}/4 = \begin{bmatrix} 1 & -1 & 1 & -1 \end{bmatrix}$

Figure A.12
Demodulation procedure

After the polar bit sequence is recovered, it is converted from the polar representation back into the original binary representation and then multiplexed into the output bit stream.

B   Calculation of the Expected Performance of the PAM Signal

B.1   For an AWGN Channel

Consider the following PAM communication system:
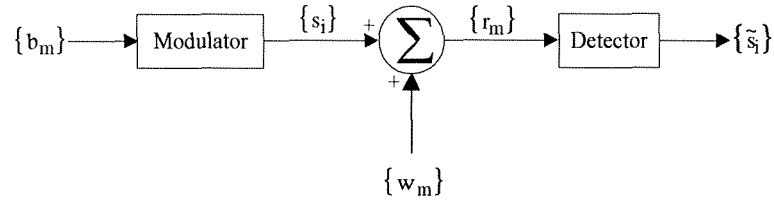
Figure B.1
PAM communication system

Where $\{b_m\}$ is a stream of binary symbols, $\{s_i\}$ is a sequence of transmitted symbols (PAM), $\{w_m\}$ is a sequence of white Gaussian noise samples, $\{r_m\}$ is a sequence of observed samples, and $\{\hat{s}_i\}$ is a sequence of estimated symbols.

Let s_i, $i = 1, \ldots, M$, be a PAM symbol that can take on M possible values, with M an arbitrary positive integer.

Let M be an odd positive integer and assume that the modulator also generates the symbol with value 0.

Consider the following signal constellation for the PAM modulator:

$$
\begin{array}{c}
i = 1 \quad 2 \qquad\qquad\qquad\qquad\qquad\qquad\qquad M\text{-}1 \quad M \\
\underbrace{\quad}_{\dfrac{-(M-1)d}{2}} \ \cdots \ \overset{}{\underset{-4d\ \ -3d\ \ -2d\ \ -d\ \ 0\ \ d\ \ 2d\ \ 3d\ \ 4d}{\quad\quad\quad\quad\quad\quad\quad}} \ \cdots \ \underbrace{\quad}_{\dfrac{(M-1)d}{2}} \ s_i
\end{array}
$$

Figure B.2
PAM constellation

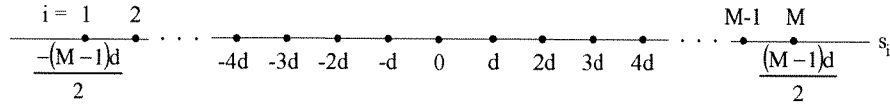Let the detector be described by an M-level quantizer and let symbol s_i be transmitted during the mth time interval. Then, the decision variable at the output of the detector is described by $r_m = s_i + w_m$, where $w_m \sim G(0, \dfrac{N_0}{2})$ and s_i takes on the values $s_i = \dfrac{(2i-1-M)d}{2}$, $i = 1, ..., M$, and d is the intra-symbol distance.

The quantizer receiver is equivalent to the minimum distance receiver. Therefore, the probability of a correct decision (cd) given that s_i was transmitted is

given by: $\quad P\{cd \mid s_i\} = \displaystyle\int_{s_i - \frac{d}{2}}^{s_i + \frac{d}{2}} \dfrac{1}{\sqrt{N_0}} e^{\frac{-(r_m - s_i)^2}{N_0}} \, d\, r_m$

$$
P\{cd \mid s_i\} = \dfrac{1}{\sqrt{2}} \int_{-\sqrt{\frac{d^2}{2N_0}}}^{\sqrt{\frac{d^2}{2N_0}}} e^{\frac{-u^2}{2}} \, d\,u = 1 - \left[\int_{-\infty}^{-\sqrt{\frac{d^2}{2N_0}}} e^{\frac{-u^2}{2}} \, d\,u = - \int_{\sqrt{\frac{d^2}{2N_0}}}^{\infty} e^{\frac{-u^2}{2}} \, d\,u \right] \left[\dfrac{1}{\sqrt{2}} \right]
$$

$$
P\{cd \mid s_i\} = 1 - 2Q\left(\sqrt{\dfrac{d^2}{2N_0}} \right), \ i = 2, ..., M\text{-}1.
$$

For i = 1: $\quad P\{cd \mid s_1\} = \displaystyle\int_{-\infty}^{s_1 + \frac{d}{2}} \dfrac{1}{\sqrt{N_0}} e^{\frac{-(r_m - s_1)^2}{N_0}} \, d\,r_m = \int_{-\infty}^{\sqrt{\frac{d^2}{2N_0}}} \dfrac{1}{\sqrt{2}} e^{\frac{-u^2}{2}} \, d\,u = 1 - Q\left(\sqrt{\dfrac{d^2}{2N_0}} \right).$

Likewise, for $i = M$: $P\{cd \mid s_M\} = P\{cd \mid s_1\} = 1 - Q\left(\sqrt{\dfrac{d^2}{2N_0}}\right)$.

Let $P_{cd} \quad P\{cd \mid s_i\}$, then $P_{cd} = \sum_{i=1}^{M} P\{cd, s_i\} = \sum_{i=1}^{M} P\{cd \mid s_i\}P\{s_i\}$.

Suppose now that symbols s_i, $i = 1, ..., M$, do not occur with equal probability. Suppose further that $P\{s_i\}$ is an even function about the origin, as in the case of a

Gaussian pdf. Then, $P_{cd} = P\left\{cd \mid s_{\frac{M+1}{2}}\right\}P\left\{s_{\frac{M+1}{2}}\right\} + 2\sum_{i=1}^{\frac{M-1}{2}} P\{cd \mid s_i\}P\{s_i\}$

$$P_{cd} = P\left\{cd \mid s_{\frac{M+1}{2}}\right\}P\left\{s_{\frac{M+1}{2}}\right\} + 2P\{cd \mid s_1\}P\{s_1\} + 2\sum_{i=2}^{\frac{M-1}{2}} P\{cd \mid s_i\}P\{s_i\}$$

$$P_{cd} = \left[1 - 2Q\left(\sqrt{\frac{d^2}{2N_0}}\right)\right]P\left\{s_{\frac{M+1}{2}}\right\} + 2\left[1 - Q\left(\sqrt{\frac{d^2}{2N_0}}\right)\right]P\{s_1\} + 2\sum_{i=2}^{\frac{M-1}{2}}\left[1 - 2Q\left(\sqrt{\frac{d^2}{2N_0}}\right)\right]P\{s_i\}$$

But, $s_{\frac{M+1}{2}} = 0$, hence

$$P_{cd} = P\{0\} + 2P\{s_1\} + 2\sum_{i=2}^{\frac{M-1}{2}} P\{s_i\} - \left[2P\{0\} + 2P\{s_1\} + 4\sum_{i=2}^{\frac{M-1}{2}} P\{s_i\}\right]Q\left(\sqrt{\frac{d^2}{2N_0}}\right).$$

The symbol error probability is therefore: $P_{se} = 1 - P_{cd} = 1 - p_1 + p_2 Q\left(\sqrt{\dfrac{d^2}{2N_0}}\right)$,

where $p_1 \equiv P\{0\} + 2P\{s_1\} + 2\sum_{i=2}^{\frac{M-1}{2}} P\{s_i\}$, and $p_2 \equiv 2P\{0\} + 2P\{s_1\} + 4\sum_{i=2}^{\frac{M-1}{2}} P\{s_i\}$.

Now, let's compute the average symbol energy E_s.

$$E_s = E\left\{s_i^2\right\} = \sum_{i=1}^{M} s_i^2 P\left\{s_i\right\} = 2\sum_{i=1}^{\frac{M-1}{2}} s_i^2 P\left\{s_i\right\} + 0^2 P\left\{0\right\} = 2\sum_{i=1}^{\frac{M-1}{2}} \frac{(2i-1-M)^2}{4} d^2 P\left\{s_i\right\}$$

$$E_s = \frac{d^2}{2} \sum_{i=1}^{\frac{M-1}{2}} (2i-1-M)^2 P\left\{s_i\right\}.$$

Let $\quad K \equiv \sum_{i=1}^{\frac{M-1}{2}} (2i-1-M)^2 P\left\{s_i\right\}.$

Then, $\dfrac{d^2}{2} = \dfrac{E_s}{K}$, and the symbol error probability can be rewritten as:

$$P_{se} = 1 - p_1 + p_2 Q\left(\sqrt{\frac{E_s}{KN_0}}\right).$$

B.2   For a Rayleigh fading plus AWGN channel

Suppose now that the same PAM signal is transmitted over a Rayleigh fading

plus AWGN channel and that coherent reception is performed on the received signal.

Then, the decision variable at the output of the detector is described by:

$$r_m = \alpha s_i + w_m,$$

where $\alpha \sim f(\alpha) = \dfrac{\alpha}{\sigma^2} e^{\frac{-\alpha^2}{2\sigma^2}}$, $\alpha \geq 0$ and $w_m \sim G(0, \dfrac{N_0}{2})$.

Note that $E\{\alpha\} = \sqrt{\dfrac{\pi}{2}}\sigma$ and $E\{\alpha^2\} = 2\sigma^2$.

The average total power of the detected signal conditioned on knowledge of α

is: $E\left\{|r_m|^2|_\alpha\right\} = \alpha^2 E\left\{s_i^2\right\} + \dfrac{N_0}{2}$.

This means that the instantaneous (conditional) SNR at the output of the

detector is: $SNR\mid_\alpha = \dfrac{\alpha^2 E\left\{s_i^2\right\}}{\dfrac{N_0}{2}} = \dfrac{2\alpha^2 E\left\{s_i^2\right\}}{N_0} = \dfrac{2\alpha^2 E_s}{N_0}$.

Let $\gamma \equiv \dfrac{\alpha^2 E_s}{N_0}$. Then the conditional symbol error probability at the output of the

detector is described by: $P\{se \mid \gamma\} = P\{se \mid \alpha\} = 1 - p_1 + p_2 Q\left(\sqrt{\dfrac{\gamma}{K}}\right)$.

Consequently, $P_{se} = \int\limits_0^\infty P\{se \mid \gamma\} f(\gamma)d\gamma = \int\limits_0^\infty \left[1 - p_1 + p_2 Q\left(\dfrac{1}{K_1}\sqrt{\gamma}\right)\right] f(\gamma)d\gamma$

$P_{se} = 1 - p_1 + p_2 \int\limits_0^\infty Q\left(\dfrac{\sqrt{\gamma}}{K_1}\right) f(\gamma)d\gamma$.

But, $\int\limits_0^\infty Q\left(c\sqrt{\gamma}\right) f(\gamma)d\gamma = \int\limits_0^\infty \left[\dfrac{1}{\pi}\int\limits_0^{\frac{\pi}{2}} e^{-\left[\frac{c^2}{2\sin^2\theta}\right]\gamma}\, d\theta\right] \dfrac{1}{\overline{\gamma}} e^{-\frac{\gamma}{\overline{\gamma}}}\, d\gamma$.

Hence, $\int\limits_0^\infty Q\left(\dfrac{1}{K_1}\sqrt{\gamma}\right) f(\gamma)d\gamma = \dfrac{1}{\pi\overline{\gamma}}\int\limits_0^{\frac{\pi}{2}}\int\limits_0^\infty e^{-\left[\frac{1}{\overline{\gamma}} + \frac{1}{2K_1^2\sin^2\theta}\right]\gamma}\, d\gamma d\theta = \dfrac{1}{\pi}\int\limits_0^{\frac{\pi}{2}} \dfrac{2K_1^2\sin^2\theta}{2K_1^2\sin^2\theta + \overline{\gamma}}\, d\theta$

$= \dfrac{1}{\pi}\int\limits_0^{\frac{\pi}{2}} \dfrac{\sin^2\theta}{\sin^2\theta + \dfrac{\overline{\gamma}}{2K_1^2}}\, d\theta = \dfrac{1}{\pi}\int\limits_0^{\frac{\pi}{2}} \dfrac{\sin^2\theta}{\sin^2\theta + \dfrac{\overline{\gamma}}{2K}}\, d\theta = \dfrac{1}{\pi}\left[\dfrac{\pi}{2} - \sqrt{\dfrac{\dfrac{\overline{\gamma}}{2K}}{1 + \dfrac{\overline{\gamma}}{2K}}}\,\tan^{-1}\left\{\sqrt{\dfrac{1 + \dfrac{\overline{\gamma}}{2K}}{\dfrac{\overline{\gamma}}{2K}}}\,\tan\left(\dfrac{\pi}{2}\right)\right\}\right]$

$$= \frac{1}{\pi}\left[\frac{\pi}{2} - \frac{\pi}{2}\sqrt{\frac{\frac{\bar{\gamma}}{2K}}{1+\frac{\bar{\gamma}}{2K}}}\right] = \frac{1}{2}\left[1 - \sqrt{\frac{\bar{\gamma}}{2K+\bar{\gamma}}}\right], \text{ where } \quad \bar{\gamma} = \frac{E_s}{N_0}E\{\alpha^2\} = \frac{2\sigma^2 E_s}{N_0}, \text{ and}$$

$$P_{se} = 1 - p_1 + \frac{1}{2}p_2\left[1 - \sqrt{\frac{\bar{\gamma}}{\bar{\gamma}+2K}}\right].$$

This result describes the symbol error probability for PAM transmission over a

single path Rayleigh fading channel when the transmitted symbols occur with a

Gaussian-like probability mass function and the total number of symbols M is odd.